3-1-2016

Elastin Like Polypeptides as Drug Delivery Vehicles in Regenerative Medicine Applications

Alex Leonard
University of South Florida, alexleonard@mail.usf.edu

Elastin Like Polypeptides as Drug Delivery Vehicles In Regenerative Medicine Applications

by

Alex Leonard

A thesis submitted in partial fulfillment
of the requirements for the degree of
Master of Science in Biomedical Engineering
Department of Chemical and Biomedical Engineering
College of Engineering
University of South Florida

Major Professor: Piyush Koria, Ph.D.
Mark Jaroszeski, Ph.D.
Nathan Gallant, Ph.D.

Date of Approval:
February 26, 2016

Keywords: Biomaterials, recombinant proteins, epidermal growth factor, protein polymers, photocrosslinking

DEDICATION

I would like to dedicate this thesis to my family for their guidance and support throughout my academic career. I would not be where I am today without their guidance. I would also like to thank my fiancé for her unconditional support.

ACKNOWLEDGMENTS

There are many people I would like to thank. To start, I want to thank my advisor, Dr. Piyush Koria, for having faith in me as an undergraduate student and letting me volunteer in his lab, which eventually turned into me being part of his lab group as a graduate student. His guidance has helped me become a better scientific investigator and will help me as I pursue a career in medicine. I would also like to thank Dr. Nathan Gallant and Dr. Mark Jaroszeski for taking the time to be a part of my thesis committee. Finally, thank you to my lab partners Raul Iglesias, Yuan Yuan, Dagmara Monfort, Tamina Johnson, and Bryce McCarthy for assisting me throughout my time in the lab.

TABLE OF CONTENTS

LIST OF TABLES

LIST OF FIGURES

ABSTRACT

Elastin like polypeptides (ELPs) are a class of naturally derived biomaterials that are non-immunogenic, genetically encodable, and biocompatible making them ideal for a variety of biomedical applications, ranging from drug delivery to tissue engineering. Also, ELPs undergo temperature-mediated inverse phase transitioning, which allows them to be purified in a relatively simple manner from bacterial expression hosts. Being able to genetically encode ELPs allows for the incorporation of bioactive peptides and functionalization of ELPs. This work utilizes ELPs for regenerative medicine and drug delivery.

The goal of the first study was to synthesize a biologically active epidermal growth factor-ELP (EGF-ELP) fusion protein that could aid in the treatment of chronic wounds. EGF plays a crucial role in wound healing by inducing epithelial cell proliferation and migration, and fibroblast proliferation. The use of exogenous EGF has seen success in the treatment of acute wounds, but has seen relatively minimal success in chronic wounds because the method of delivery does not protect exogenous EGF from degradation, or prevent it from diffusing away from the application site.

We created an EGF-ELP fusion protein to combat these issues. As demonstrated through the proliferation of human skin fibroblasts *in vitro*, the EGF-ELP may be able to aid in the treatment of chronic wounds. Furthermore, the ability of the EGF-ELP to self-assemble near physiological temperatures could allow for the formation of drug depots at the wound site and minimize diffusion, increasing the bioavailability of EGF and enhancing tissue regeneration.

The objective of the second study was to create an injectable hydrogel platform that does not require conjugation of functional moieties for crosslinking or biological activity. Hydrogels are three-dimensional polymer networks that are able to absorb water and biological fluids without dissolving. Their high water content gives them physical properties similar to soft tissues, making them useful as scaffolds for cell migration and drug delivery vehicles. Injectable hydrogels that crosslink *in situ* are particularly useful because they can form to the shape of the defect, providing a near perfect fit. However, many hydrogel platforms cannot be crosslinked *in situ* because cytotoxic crosslinking reagents are required. Additionally, hydrogels typically require the chemical conjugation of crosslinking domains and bioactive peptides to the polymer backbone, adding more steps and time required for hydrogel production.

We devised an injectable hydrogel platform that can be synthesized in a single step using photoreactive ELPs as the polymer backbone. Leucine auxotrophic *Eshcherichia coli* expressed ELPs containing photoleucine, a leucine analog and photoreactive diazirine crosslinker, which is substituted for leucine periodically throughout the ELP sequence. Upon exposure to ultraviolet radiation (~370 nm), photoleucine is able to form covalent crosslinks with amino acid side chains, forming a polymer network for hydrogel formation. Additionally, recombinant growth factors and morphogens can be encoded into the ELP sequence providing a simple method of hydrogel functionalization for regenerative medicine applications.

The potential for this platform was demonstrated through *in vivo* crosslinking of photoreactive ELPs in the expression hosts. Though the production of the photoreactive ELP was not as forthright as originally assumed. The substitution of noncanonical amino acids typically requires the auxotrophic expression hosts to be starved of the amino acid that they are auxotrophic for. A noncanonical analog of said amino acid can then be supplemented into

expression media, maximizing incorporation. In this investigation, it was found the addition of photoleucine alone inhibited photoreactive ELP expression. ELP expression only occurred in the presence of photoleucine if valine or leucine was also present in the media. Furthermore, valine was found to aid the production of ELPs as much as leucine. It was postulated the bacterial translational machinery might need to be altered for optimal ELP expression.

CHAPTER 1: ELASTIN LIKE POLYPEPTIDES

Elastin is an extracellular matrix protein commonly found in the connective tissue of the skin, ligaments, blood vessels, and lungs. Elastin provides these tissues with important physical properties that allow them to function properly, primarily the ability to extend and elastic recoil [1]. The precursor to the elastin polymer is tropoelastin, a monomer that contains hydrophobic and hydrophilic domains which can be crosslinked via lysine residues. The crosslinked tropoelastin monomers form insoluble elastin fibers [2].

Elastin like polypeptides (ELPs) are a class of recombinant proteins whose sequences are derived from the hydrophobic domain of tropoelastin. A common sequence used in ELPs is $(VPGXG)_n$, where X is any guest residue other than proline (introduction of proline as the guest residue prevents ELPs from inverse phase transitioning) [3] and *n* is the number of pentapeptide repeats. This sequence is genetically encodable, allowing the guest residue and number of pentapeptide repeats to be altered to give the ELP particular characteristics [2].

The $(VPGXG)_n$ sequence allows ELPs to undergo inverse phase transitioning, an entropically driven phenomena that allows ELPs to solubilize in solution below their transition temperature (T_t) and form insoluble aggregates above their T_t (Figure 1, next page) [2, 4]. The formation of aggregates above the T_t is driven by the decreased organization of the solvent shell above the T_t, shown in Figure 1 (next page). As a result of this change in entropy, the hydrophobic portions of the ELPs collapse on one another, creating an ELP aggregate [4]. Additionally, the phase transition is reversible, allowing ELPs to transition between the two phases depending on the temperature. The ability for ELPs to undergo reversible inverse phase

transitioning can be exploited to purify the protein in a process known as inverse transition cycling (ITC), a process where the protein is purified through a series of centrifugations below and above the T_t [2].

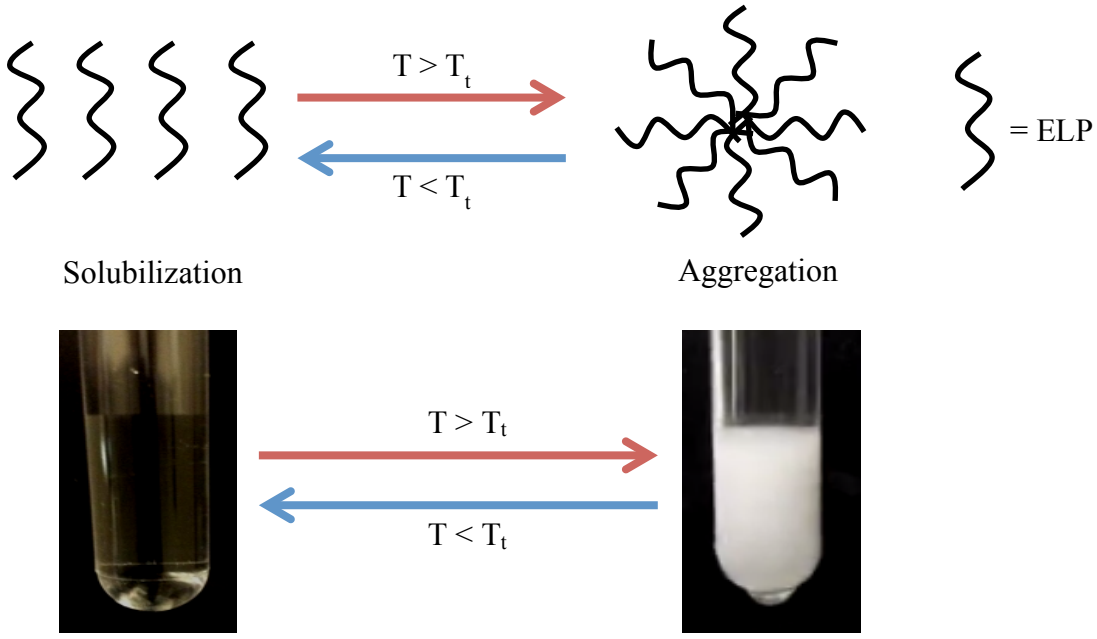

Figure 1 Inverse phase transition of ELPs. When below the transition temperature ($T<T_t$) ELPs are soluble in solution. When the temperature is increased above the transition temperature ($T>T_t$) ELPs become insoluble and form aggregates.

While there are synthetic materials that also have the ability to undergo inverse phase transitioning, ELPs do possess advantages over synthetic materials. The primary benefit is the ability to genetically encode the ELP sequence, giving researchers complete control over the chemical composition, and thus the physical characteristics of the ELP. For instance, by simply changing the guest residue, ELP thermal characteristics can be modified [2]. It has been demonstrated that when hydrophobic amino acids are substituted as the guest residue, the T_t is depressed. Conversely, when charged or polar amino acids are substituted in the place of the guest residue the T_t is elevated [5]. In addition to control over the thermal response of ELPs, having the ability to manipulate the identity of the guest residue allows for incorporation of

reactive amino acids or amino acid analogs which can be used for conjugation of biological agents or crosslinking [2].

1.1 Recombinant DNA Techniques to Construct ELP Genes

As aforementioned, ELPs are a class of genetically encodable biopolymers containing a repetitive sequence of the pentapeptide repeat $(VPGXG)_n$. The production of ELPs, and other protein-based polymers, requires the same five steps: (1) Construction of the plasmid to be used for protein expression, (2) transformation of the constructed plasmid into cloning competent cells, (3) verification that the plasmid has been transformed into cloning competent cells and that no mutations have occurred within the plasmid, (4) transformation of the expression plasmid into expression competent cells, and finally (5) protein expression and purification. The first step, constructing the plasmid, can present problems for proteins that contain repetitive peptide sequences, such as ELPs. The main issue is creating a gene for a large protein sequence from a small gene fragment [6].

For instance, the gene for the ELP V_{50} contains a nucleotide sequence that encodes for 50 repeats of the pentapeptide VPGVG. Typically, the V_{50} gene would be constructed from a smaller gene fragment, possibly a gene encoding five pentapeptide repeats of VPGVG (V_5). There are a multitude of methods used to synthesize large gene fragments from smaller gene fragments; however, two of the more common techniques used for ELP gene construction are concatemerization and recursive directional ligation.

1.1.1 Concatemerization

Concatemerization entails the ligation of a random number of identical monomeric gene fragments to one another, though the number of monomers ligated can be highly influenced by reaction conditions. This method is able to generate a collection of oligomeric genes composed

of identical monomers during a single ligation. For concatemerization to be implemented, the monomeric gene fragment to be self-ligated must contain single stranded overhang sequences at the monomer's head and tail that are the same length and complementary, but not identical. Essentially, the overhang sequences must be cohesive, but nonpalindromic. This ensures the monomers are ligated in a head-to-tail fashion, as opposed to a head-to-head or tail-to-tail manner, which could alter the encoded amino acid sequence [6]. Concatemerization has been widely used to construct plasmids for repetitive amino acid sequences. For instance, concatemerization was used by Cappello et al when constructing a gene for a silk-like protein that contained 160 repeats of the hexapeptide sequence GAGAGS [7].

To create the cohesive nonpalindromic overhangs, endonucleuase digestion via restriction enzymes can be used. For instance, one of the more widely used restriction enzymes, *Ban* I, recognizes the six base-pair sequence 5'-G/GTGCC (*Ban* I cleaves the sequence at the /). To ensure head-to-tail ligation occurs, the monomer sequence that is to be oligomerized can be flanked by the *Ban* I restriction site. The 5' head and 5' tail produced upon cleavage with *Ban* I will contain cohesive nonpalindromic sequences, which will result in head-to-tail ligation [8]. In addition, it has been demonstrated by McPherson et al that using restriction enzymes with the ability to recognize interrupted palindromes can be used to make certain that head-to-tail ligations takes place [9]. Figure 2 (next page) illustrates the construction of a gene library using concatemerization.

As aforementioned, concatemerization has proven to be a valuable technique for generating different sized polypeptides that contain repeats of identical monomeric sequences during a single ligation; however, there are major limitations when using this technique. One major shortcoming is the lack of precise control over the number of monomers that ligate;

though, this is only an issue when there is a need for precise control over the number of monomeric repeats present in the new gene. Another drawback is there is no control over the sequence generated by ligation of the monomers, which is why concatemerization can only be conducted using identical monomers [6]. However, there are other recombinant DNA techniques that are able to overcome these drawbacks, such as recursive directional ligation.

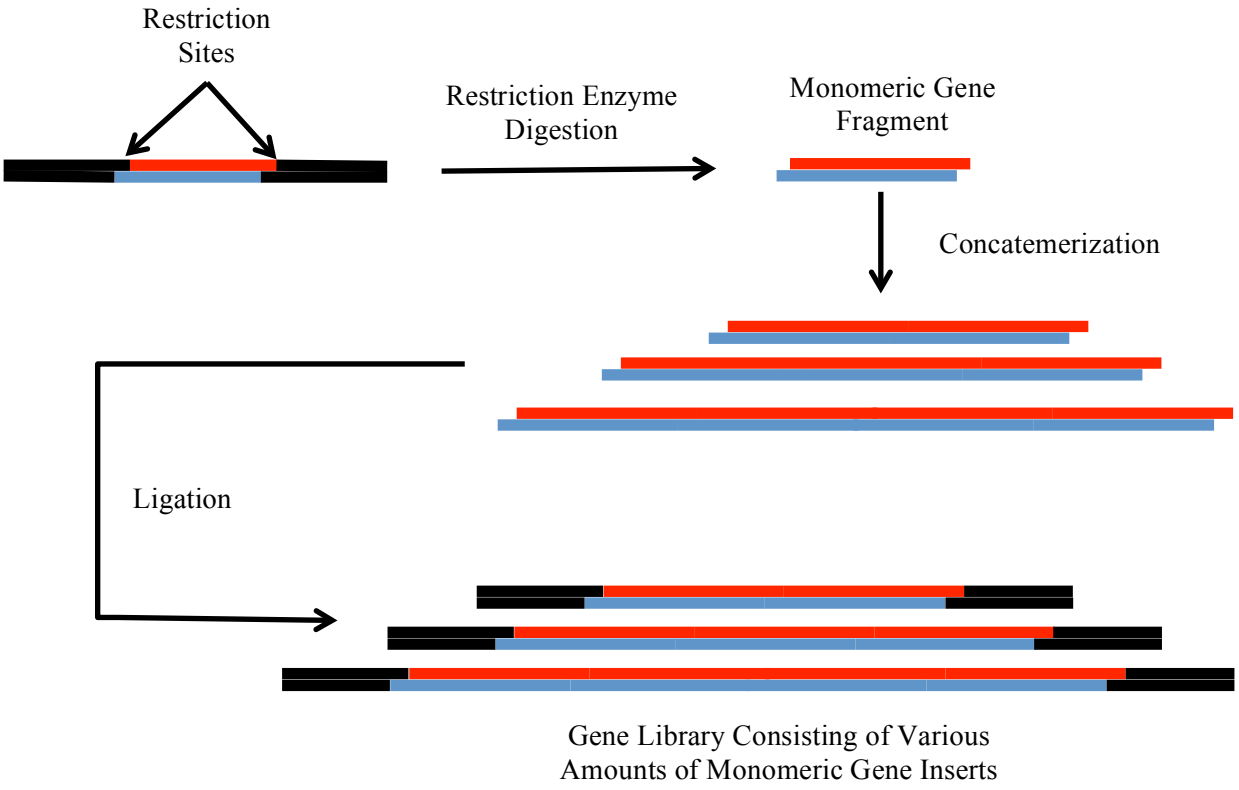

Figure 2 Creating gene libraries via concatemerization. Following restriction enzyme digestion, the monomeric gene fragment undergoes concatemerization to produce a library of genes containing various numbers of monomeric gene fragments.

1.1.2 Recursive Directional Ligation

Similar to concatemerization, recursive directional ligation (RDL) is a recombinant DNA technique used to construct genes for peptides containing repetitive amino acid sequences. Both methods utilize head-to-tail ligation to produce genes and make use of restriction enzymes that cleave interrupted palindrome sequences. However, there are several differences between the

two techniques. Unlike concatemerization, RDL allows for precise control over the number of monomeric repeats inserted into the gene and the sequence in which monomers are inserted into the gene. Hence, RDL is used to construct genes encoding repetitive polypeptides that must be a specified size and sequence [6].

Typically, the same procedure is followed when using RDL, regardless of the number of peptide repeats or the sequence. To start, the monomer gene encoding the peptide sequence to be oligomerized is ligated into a cloning vector in such a way that the monomer gene is flanked by two different restriction enzyme recognition sites (RE1 and RE2). To begin oligomerization, the monomer gene is removed from the cloning vector using RE1 and RE2. Additionally, a separate aliquot of the cloning vector containing the monomer gene is cut using either RE1 or RE2, producing a linearized vector. The monomer insert can then be ligated in a head-to-tail fashion into the linearized vector. This procedure can be repeated until the desired number of peptide repeats has been inserted [10]. Figure 3 (next page) demonstrates the general procedure used for RDL.

Additionally, a gene containing a different peptide sequence can be ligated into the linearized vector as long as the overhang sequences are cohesive and nonpalindromic in relation to the linearized vector [6]. While RDL can be tedious when creating genes containing large numbers of monomeric gene fragment repeats, the ability to control the number of monomeric gene fragments ligated into the vector and insert gene fragments encoding different peptide sequences makes RDL particularly useful for the construction of ELP genes, as demonstrated by Meyer and Chilkoti [10]. Furthermore, a combination of concatemerization and RDL can be used to synthesize genes containing multiple repeats of monomeric gene fragments.

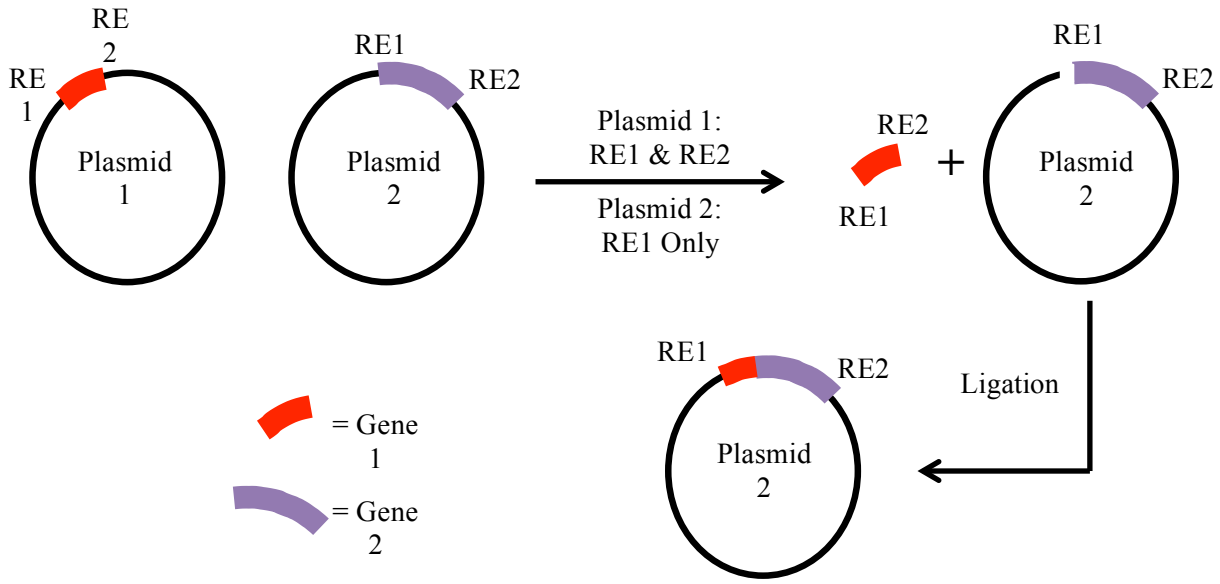

Figure 3 Plasmid construction using recursive directional ligation (RDL). A gene composed of Gene 1 and Gene 2 can be designed using RDL. Restriction sites are conserved while no additional restriction sites are formed.

1.2 Recombinant Protein Purification

1.2.1 Affinity Chromatography

One of the most common processes used to purify recombinant proteins is affinity chromatography [10]. Affinity chromatography is a liquid chromatographic technique that utilizes nonbiologcal or biological interactions to isolate specific compounds from complex solutions [11]. The reactions are highly specific and are normally reversible, similar to an antibody-antigen interaction [12].

In affinity chromatography, an affinity ligand specific for the target compound is immobilized on a solid phase, and the liquid solution containing the desired compound is passed over or through the immobilized phase. As the solution passes through the immobilized phase, the binding agent will bind the desired product and isolate it from the solution. The target compound is then eluted from the ligand and immobilized phase using one of two methods. Specific elution is a method that weakens the target-ligand interaction by competing for the

ligand or target compound, eventually leading to the target compound being released from the ligand. Nonspecific elution aims to decrease the association constant between the target compound and ligand by altering the environmental conditions surrounding the complex. This can be done by manipulating the salt concentration or pH to reduce hydrogen bonding, hydrophobic interactions, and electrostatic interactions [12].

Affinity chromatography has been used to purify ELPs that do not retain the inverse transition property. For example, ELPs can be labeled with a His-tag, which can be used to purify the protein via metal-ion affinity chromatography [13]. While affinity chromatography can be used for laboratory-scale protein purification, there are economical and technical limitations the make it difficult to scale-up to high capacity applications [10].

1.2.2 Inverse Transition Cycling

Inverse transition cycling (ITC) is a protein purification method that utilizes the inverse phase transitioning property of ELPs. ITC provides many economic and technical benefits over other protein purification methods, such as affinity chromatography [10]. During ITC, ELPs are isolated from the bacterial cell lysate in a series of hot centrifugations (above the T_t) and cold centrifugations (below the T_t). When a cold centrifugation is conducted, the ELP is solubilized and insoluble impurities can be removed [2]. Reducing agents (such as DTT) can be added prior to the cold centrifugation if the ELP contains cysteines that are able to form disulfide bonds. The formation of disulfide bonds may reduce the solubility of ELP in solution, thus the reduction of disulfide bridges is crucial for purifying cysteine-containing ELPs [14]. The supernatant containing the ELP is then heated above the T_t and undergoes a hot centrifugation. During the hot centrifugation the ELP transitions to form an insoluble aggregate, which forms a pellet, isolating the ELP from soluble impurities that are present in the solution. Additionally, salt can

be added to the supernatant prior to the hot centrifugation to lower the T_t, thus aiding in the formation of the insoluble ELP aggregate [2].

After the hot centrifugation, the ELP pellet can be resuspended in cold buffer if additional ITC cycles need to be completed, or DI water if the ITC process is complete. It typically takes multiple cycles of ITC to purify the ELP to sufficient levels [2]. After resuspension in DI water, the ELP solution is dialyzed against DI water for 18-24 hours to remove any salts or reducing agents that may be present. The ELP is then lyophilized so that it can be stored at room temperature. The ITC process is described in Figure 4 (below).

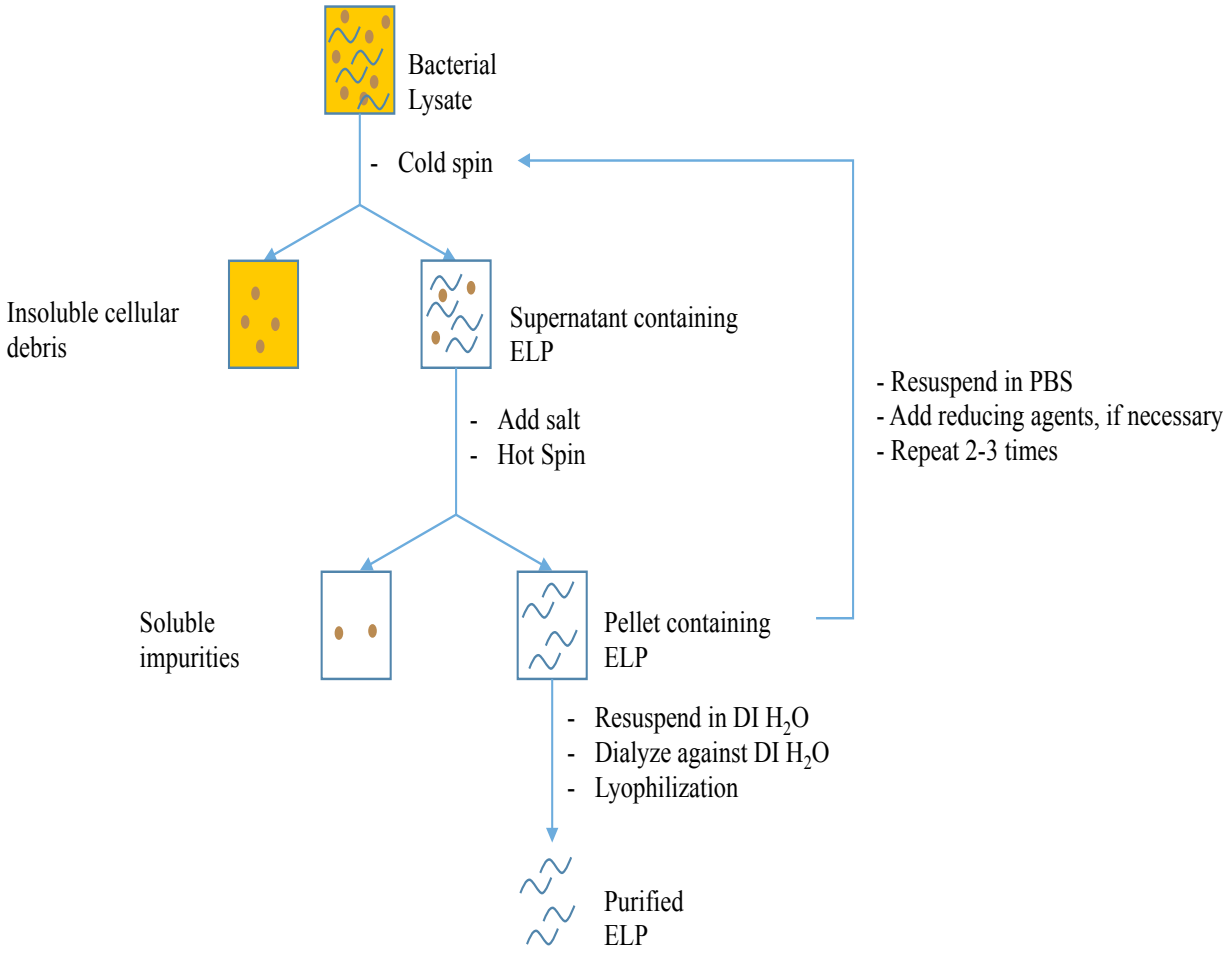

Figure 4 Inverse transition cycling (ITC). ELPs are purified through series of cold and hot centrifugations. Salts can be added to aid ELP precipitation while reducing agents can increase ELP solubility.

1.3 Elastin Like Polypeptides in Biomedical Applications

Due to their high level of tunability and biocompatibility, ELPs are beginning to show great value in variety of biomedical applications, such as drug delivery and tissue engineering applications [15-17]. For instance, bioactive peptides, such as growth factors, have been fused to ELPs and have been shown to retain the biological activity of the growth factor. These growth factor-ELP (GF-ELP) fusion proteins have been also been shown to possess the inverse phase transition property of ELPs. This provides a simple method for the production and purification of growth factors, and can also aid in growth factor delivery as the self-aggregation of GF-ELPs can increase the bioavailability of GFs [18].

As aforementioned, ELPs can also be functionalized by substituting reactive amino acids in the ELP sequence at the guest residue position. For example, cysteine and lysine have been substituted to enable crosslinking and drug conjugation to ELPs [14, 19]. Though, this is not limited to canonical amino acids. Reactive noncanonical amino acid analogs can also be incorporated in the ELP sequence using auxotrophic expression hosts and expression media supplemented with the noncanonical analog. For example, incorporation of photoreactive noncanonical amino acid analogs can enable crosslinking of ELPs upon exposure to ultraviolet radiation [20]. In this thesis, we aimed to exploit the fact ELPs can be functionalized by simply altering the ELP sequence to create innovative drug delivery platforms.

CHAPTER 2: DEVELOPMENT OF EPIDERMAL GROWTH FACTOR-ELASTIN LIKE POLYPEPTIDE FUSION PROTEIN

2.1 Introduction

2.1.1 Epidermal Growth Factor and the Epidermal Growth Factor Receptor

Epidermal growth factor (EGF) is a 53 amino acid single-chain polypeptide discovered by Dr. Stanley Cohen in 1962 while studying the effects of mice submaxillary gland extract on newborn mice [21, 22]. EGF is a member of a family of growth factors, the EGF family, that are able to bind to the epidermal growth factor receptor (EGFR), a tyrosine kinase transmembrane protein found throughout the epidermis, especially in the basal layer. Upon binding EGF, the EGFR undergoes dimerization and autophosphorylation, activating the mitogen-activated protein kinase pathway (MAPK). Ultimately, activation of the MAPK pathway influences the phosphorylation of various transcription factors and calcium release of protein kinase C [23].

Also, activation and dimerization of the EGFR due to EGF binding has been shown to play a crucial role in epidermal regeneration and corneal epithelial regeneration through enhancing epithelial cell proliferation and migration, stimulating the production of extracellular matrix proteins, and increasing fibroblasts proliferation [23].

2.1.2 Epidermal Growth Factor and Regenerative Medicine

The use of exogenous EGF in acute wound healing was originally examined in 1973 by Savage and Cohen, when they demonstrated corneal epithelial hyperplasia can be induced using EGF [24]. Since then, the use of exogenous EGF has shown promise in the treatment of acute surgical wounds in rabbits [25], corneal epithelial wounds [26-28], and partial thickness burn

wounds [29]. However, the use of exogenous EGF to aid in the treatment in chronic wounds, such as diabetic ulcers or venous ulcers, has not been as successful.

Exudative fluid withdrawn from chronic wounds has shown, compared to acute wounds, an increased level in protease activity and diminished EGF activity [30, 31]. This hints at the possibility that EGF is degraded by excessive protease activity within the microenvironment of chronic wounds. As demonstrated by Falenga *et al.*, the topical administration of aqueous EGF solutions to venous ulcers can increase the rate of re-epithelialization and decrease wound size when compared to control groups. However, the results were not statistically significant, and were not nearly as prominent as results seen in acute wounds [32]. Due to this, alternative delivery systems have been investigated.

As aforementioned, the microenvironment in chronic wounds leads to the excessive degradation of growth factors that enter the wound. The high rate of degradation means there is not a high enough concentration of EGF present at the wound site to make a significant difference in healing, and the growth factor is not present in the wound long enough for its presence to be detected [33]. Additionally, when EGF is administered using simple bolus delivery methods, such as topical application [32] or intralesional injections [34], it is able to easily diffuse away from the wound decreasing the local concentration of EGF, thus minimizing its impact on wound healing. This can lead to using large quantities of EGF and having to reapply the treatment continuously, potentially leading to tumor development and making the therapy expensive [33].

To combat these issues, delivery systems utilizing hydrogels with EGF encapsulated within the polymer network have been investigated. While there has been moderate success using this method, there is little control over the release of EGF from the polymer network,

resulting in a burst release profile of EGF [35]. While there may be some instances where a burst release profile is preferred, most applications require the ability to control the release of EGF to ensure the growth factor is present throughout the healing process [26]. To achieve this, growth factor delivery vehicles that will allow for the covalent binding, or at least physical interactions, between growth factors and a scaffold will need to be developed.

2.1.3 Utilization of ELP Fusion Proteins for Drug Delivery

The biocompatibility and ability to self-assemble associated with ELPs makes them ideal for *in vivo* applications. Additionally, since ELPs are genetically encodable, it is relatively simple to fuse other biologically significant peptides to ELPs creating ELP fusion proteins, as illustrated in Figure 5 (below). These ELP fusion proteins have been shown to retain not only the inverse phase transition property of traditional ELPs, but also the biological activity of the fused peptide [18]. Hence, ELP fusion proteins have the potential to serve as all-in-one drug delivery systems, containing the drug and delivery vehicle without the need for chemical conjugation.

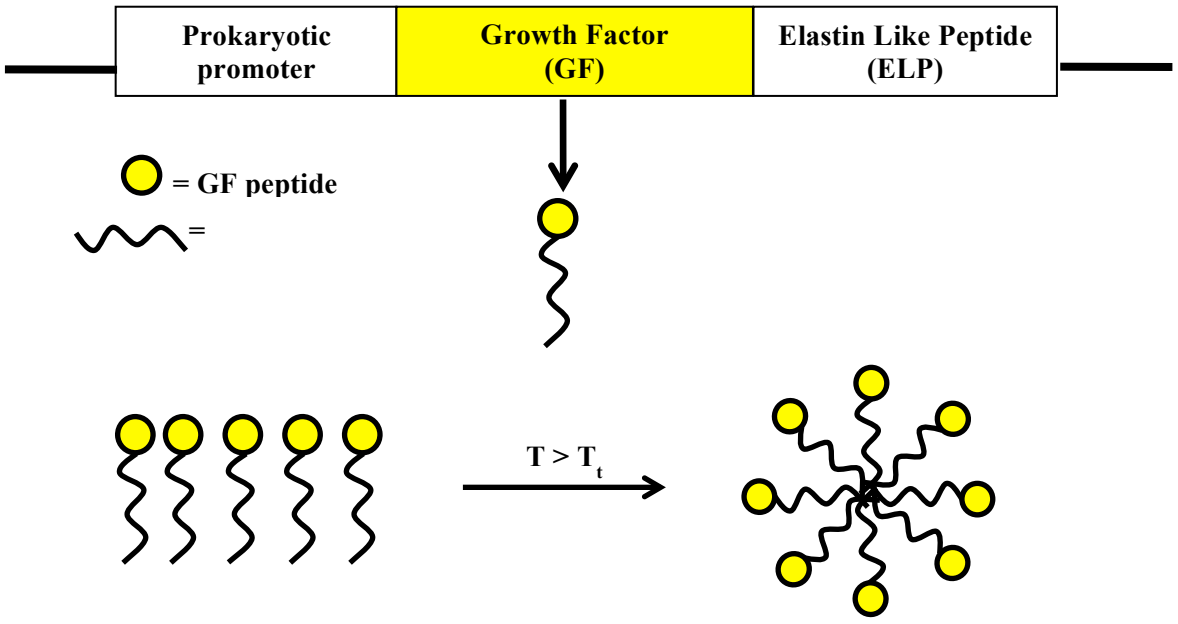

Figure 5 GF-ELP gene design and aggregation. The top of figure shows the sequence the genes are in when inserted into the expression vector. At the bottom, the aggregation of GF-ELP fusion proteins above their T_t is illustrated.

The ability to create ELP fusion proteins that retain the biological activity of peptides and the inverse phase transition property of ELPs makes them ideal candidates for localized drug delivery. There are a number of ways ELP fusion proteins can be utilized for local drug delivery. One method has seen the creation of coacervate drug depots via aggregation of ELP fusion proteins for treatment of osteoarthritis [36] and neuroinflammation [37]. Furthermore, keratinocyte growth factor-ELP fusion protein coacervates have been used in conjunction with fibrin hydrogels for delivery of keratinocyte growth factor-ELP fusions to wounds in animal models [18]. Another method utilized for the local delivery of ELP fusion proteins is chemically crosslinking ELP domains to create a three-dimensional scaffold [38].

2.2 Project Objective

The aim of this project was to create a biologically active EGF-ELP fusion protein that could address the issues connected with the use of exogenous EGF in regenerative medicine. Currently, the administration of exogenous EGF is carried out by either a simple injection or topical application. Unfortunately with these techniques, EGF can be rapidly degraded and can diffuse away from the application site with relative ease, leading to a decreased local concentration of EGF and minimal improvements as far as tissue regeneration is concerned.

The EGF-ELP fusion protein produced was meant to address these complications. By creating an EGF-ELP fusion protein, the biological activity of EGF should be kept intact while the characteristics of ELPs are also maintained, meaning the EGF-ELP fusion protein will be able to self-assemble near physiological temperatures making it an ideal vehicle for the local delivery of EGF to wounds. To investigate the potential use for the EGF-ELP in regenerative medicine, the fusion protein was purified, and its thermal and biological properties were analyzed.

2.3 Materials and Methods

2.3.1 Materials

EGF and $V_{40}C_2$ (ELP) genes were purchased from GenScript. Restriction enzymes and other enzymes used for cloning were purchased from New England Biolabs. For purification of DNA after gel electrophoresis, a gel extraction kit produced by Qiagen was used. For cell culture purposes, fetal bovine serum (FBS) and Dulbecco's Modified Eagle's Medium (DMEM) were purchased from Life Technologies, and antibiotic-antimycotic (AA) solution was purchased from Corning CellGro. Dr. Eric Haura from Moffitt Cancer Center generously donated A549 adenocarcinomic alveolar basal epithelial cells and A431 epidermoid carcinoma cells. Human skin fibroblast were purchased from ATCC. Ethidium homodimer was purchased from Life Tehnologies. Fluorescent photographs for migration and cell counting experiments were taken using an EVOS® FL Digital Inverted Microscope. An Eon ™ High Performance Microplate Spectrophotometer (Biotek) was used for optical density readings at 350 nm (OD350), while a Synergy Multi-Mode Reader (Biotek) was used for fluorescence readings during A549 and fibroblasts proliferation studies. Dynamic light scattering was conducted using a Zetasizer Nano S (Malvern, UK).

2.3.2 EGF-ELP Gene Construction

The EGF gene (amino acid sequence in Appendix A) was sent in a pUC57 plasmid with *PflM*I and *Bgl*I restriction enzyme sites flanking the gene. *PflM*I and *Bgl*I were used to remove the EGF gene from the pUC57 plasmid, and *Bgl*I was used to linearize the ELP pUC19 plasmid. After digesting the plasmids with the required restriction enzymes, gel electrophoresis was used to separate DNA fragments. The EGF gene and linearized ELP gene were purified using a gel extraction kit**.** Once both genes were purified from the gel, the EGF gene was ligated into the

linearized ELP pUC19 plasmid and transformed into Top10*f* competent cells (Invitrogen). The ligation was carried out so that EGF was at the N-terminus of the fusion protein. Polymerase chain reaction (PCR) was used to ensure the EGF gene was successfully ligated into the linearized ELP pUC19 plasmid. Figure 6 (below) illustrates the process of creating the EGF-ELP pUC19 vector.

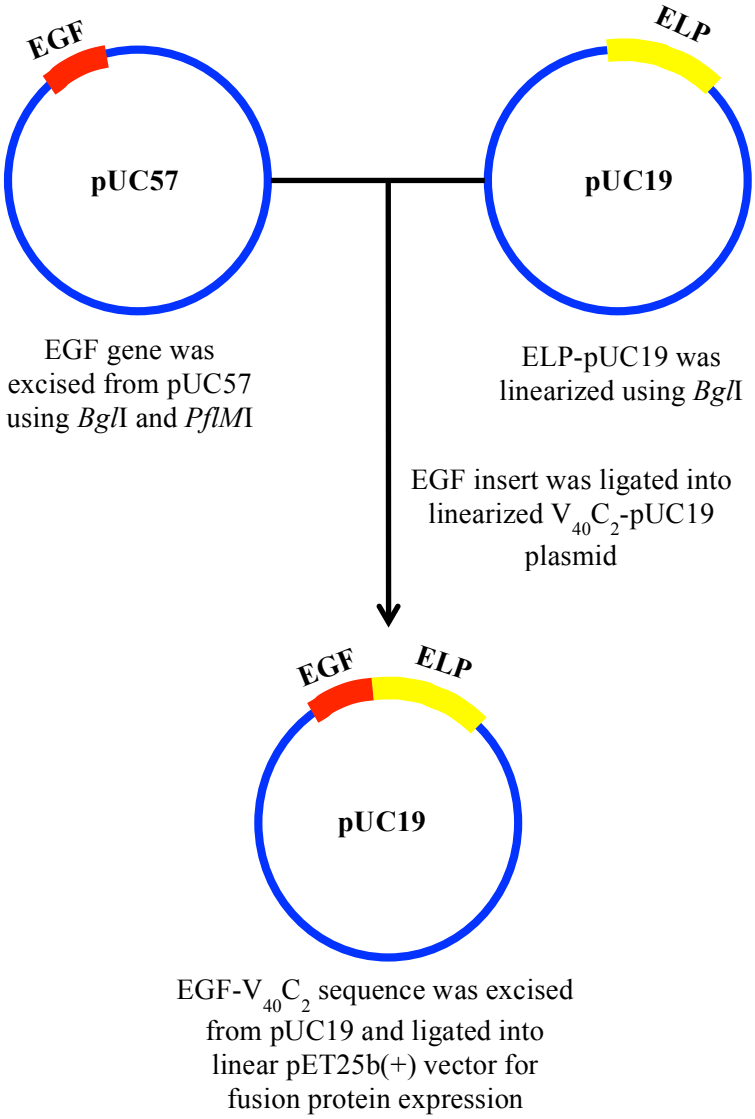

Figure 6 Producing the EGF-ELP fusion protein gene. The EGF gene was excised and inserted into a linearized ELP-pUC19 cloning vector. Once the EGF-ELP pUC19 vector was created, the EGF-ELP gene fragment was excised and ligated into a linearized expression vector for ELP expression.

The EGF-ELP pUC19 plasmid was then cut using the restriction enzymes *Pfl*MI and *Bgl*I to excise the EGF-ELP gene. The EGF-ELP gene was purified using the same gel extraction method described previously. The isolated EGF-ELP gene was then ligated into a linearized pET25b(+) expression vector and transformed into Top10*f* competent cells. PCR was again used to ensure the EGF-ELP gene was successfully ligated into the pET25b(+) expression vector. The EGF-ELP pET25b(+) vector was sent for sequencing to confirm the EGF-ELP gene was successfully ligated and no mutations were present. The EGF-ELP pET25b(+) vector was then transformed into BLR(DE3) competent cells (Invitrogen) for expression.

2.3.3 EGF-ELP Expression and Purification

Escherichia coli BLR(DE3) competent cells containing the EGF-ELP pET25(b+) plasmid were cultured in 50 mL of TB media (yeast extract: 24 g/L, tryptone: 12 g/L, potassium phosphate monobasic: 2.31 g/L, potassium phosphate monobasic: 12.54 g/L, proline: 11.5 g/L, glycerol: 4 ml/L, and carbenicillin: 100 μg/ml) overnight. The next day, the starter culture was added to 1 L of fresh TB media and cultured for 18 hours at 37°C and 180 RPM. *E. coli* was collected by centrifugation (3,000 G's, 4°, 20 minutes) and resuspended in 160 mL of 4°C phosphate buffered saline (PBS). Bacteria was then lysed using a Model 505 Sonic Dismembrator (Fisher Scientific) set to run at 50% amplitude for 12 minute cycles (3 cycles total, pulse on 59 seconds, pulse off 59 seconds). After each cycle, the bacterial lysate was cooled at 4°C for 40 minutes. To remove cellular debris, the bacterial lysate was centrifuged (20,000 G's, 4°C, 20 minutes) and the supernatant containing EGF-ELP was collected.

After collecting the supernatant, EGF-ELP was purified using inverse temperature cycling (ITC). The supernatant was supplemented with 1 M NaCl and placed in a water bath at 45°C for 40 minutes. The EGF-ELP solution underwent a hot spin (20,000 G's, 40°C, 10

minutes), after which the supernatant was discarded and the pellet was resuspended in 100 mL PBS containing 10 mM dithiothreitol (DTT) at 4°C. DTT served as a reducing agent to prevent the formation of disulfide bonds, which would decrease the solubility of the EGF-ELP. Prior to cold spins (20,000 G's, 4°C, 20 minutes), the EGF-ELP solution was cooled at 4°C for 1 hour. The cycle of hot and cold spins was conducted 3 times, or until cellular debris was no longer visible after centrifugation. After the last hot spin, the EGF-ELP pellet was resuspended in 50 mL deionized (DI) H_2O at 4°C. The EGF-ELP solution was then dialyzed against DI H_2O for 18 hours at 4°C to remove any salts or DTT that may be present. After dialysis, the EGF-ELP was lyophilized.

2.3.4 Total Protein Stain and Western Blot Analysis

Total protein stains and western blot analysis were conducted using sodium dodecyl sulfate polyacrylamide gel electrophoresis (SDS-PAGE). Samples were taken from various stages of ITC and were analyzed by SDS-PAGE (12% acrylamide gels). For western blots, anti-EGF antibody (Cell Signal) was used to label EGF-ELP. Horseradish peroxidase linked (HRP) anti-rabbit antibody (Cell Signal) was used to label anti-EGF antibody, and a chemiluminescent signal was produced using LumiGLO ® Reagent and peroxide (Cell Signaling Technologies).

2.3.5 EGF-ELP Transition Temperature

EGF-ELP was dissolved in cold PBS (~4°C) to create a 5 μM solution and was then filtered using a 0.45 μm filter. Dynamic light scattering (DLS) was used to analyze the sample as the temperature was increased from 10°C to 40°C in 5°C increments. The sample was allowed to equilibrate for 15 minutes once the DLS apparatus reached the desired temperature. Once the sample had equilibrated, the DLS apparatus analyzed the EGF-ELP sample and recorded the derived count rate (kcps) twice at each temperature.

2.3.6 Elastic Behavior of EGF-ELP

EGF-ELP was diluted in cold PBS (~4°C) to a concentration of 15 μM. 100 μl was then loaded in a round bottom 96 well plate, which was then placed in the spectrophotometer. The optical density at 350 nm (OD 350) was measured as the EGF-ELP solution was heated from 26°C to 42°C in increments of 2°C. The OD 350 was also measured as the solution was cooled from 42°C to 26°C in increments of 2°C. The EGF-ELP solution was shaken for 30 seconds and allowed to equilibrate for 10 minutes at each temperature before the OD 350 was measured.

2.3.7 EGF-ELP Size Characterization

A 5 μM EGF-ELP solution was prepared using cold PBS (~4°C) and filtered using a 0.45 μm filter. DLS was used to analyze the EGF-ELP solution at 15°C (below the T_t) and 37°C (above the T_t). The EGF-ELP sample equilibrated at each temperature for 15 minutes prior to being analyzed. After equilibration, the EGF-ELP solution was analyzed three times at each temperature. The particle size distribution (mean intensity) and polydispersity index (PDI) were calculated by the Zetasizer Nano S software.

2.3.8 A549 Proliferation and Migration

For the A549 proliferation study, A549 cells were seeded in a 48 well plate at 15,000 cells/well in DMEM + 10% FBS + 1% AA for 24 hours. Next, cells were washed with 1x PBS and serum starved for 24 hours. Cells were then treated with serum free media, and various amounts of ELP, EGF-ELP, and recombinant EGF (rEGF) for 48 hours. 24 hours into treatment, bromodeoxyuridine (BrdU) was added to the wells. After 48 hours, a BrdU assay was conducted to determine the amount of BrdU incorporated into newly synthesized DNA by measuring the fluorescence at 450 nm.

For the migration experiment, cells were prepared by seeding 10,000 cells/well in DMEM + 10% FBS + 1% AA. After 24 hours cells were washed with 1x PBS and serum starved for an additional 24 hours. Following serum starvation, cells were treated with EGF-ELP or ELP (5 μM). After 48 hours of treatment, cells were treated with calcein and incubated at 37°C for 30 minutes. After incubation, photographs were taken at 10x and 20x.

2.3.9 Inhibition of A431 Proliferation

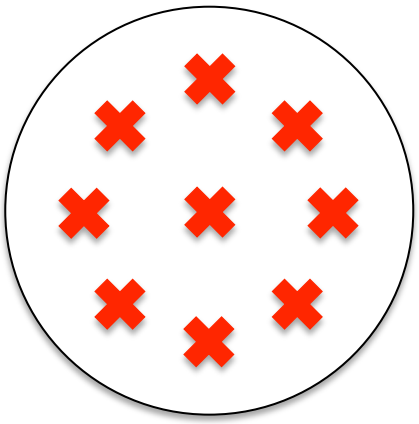

Figure 7 Picture locations in 48 well plate. After staining with NucBlue and ethidium homodimer, and 30 minutes of incubation at 37°C pictures were taken at 10x at the described locations in wells.

A431 epidermoid carcinoma cells were seeded in a 48 well plate at 10,000 cells/well in DMEM + 10% FBS + 1% AA for 24 hours. Cells were then washed with 1x PBS and cultured in 2% FBS for 24 hours. After 24 hours, cells were treated with different concentrations of ELP and EGF-ELP in 2% FBS for 48 hours. Cell nuclei were then stained with NucBlue (2 drops/ml media) (Life Technologies) and dead cells were stained with ethidium homodimer (1:500 dilution). Cells were then incubated at 37°C for 30 minutes. 9 pictures/well were taken at 10x magnification as shown in Figure 7 (above). Images were then analyzed using ImageJ software and a macro created by Raul Iglesias.

2.3.10 Human Skin Fibroblast Proliferation

Human skin fibroblast were seeded in a 48 well plate with 20,000 cells/well in DMEM + 10% FBS + 1% AA. After 24 hours, cells were serum starved in DMEM + 1% AA for 48 hours. Following serum starvation, cells were treated with various amounts of EGF-ELP, ELP, and recombinant EGF (rEGF), for 48 hours in serum-free culture. Following treatment, cell proliferation was measured using a Hoescht assay. Fluorescence changes were recorded using an excitation wavelength of 360 nm and an emission wavelength of 460 nm.

2.3.11 Statistical Analysis

Statistical significance for biological activity assays was determined using the p-value calculated from ANOVA.

2.4 Results

2.4.1 EGF-ELP is Purified Using Inverse Transition Cycling

The total protein stain displayed in Figure 8 (next page) shows the total protein content from multiple phases throughout the inverse transition cycling (ITC) purification process. Table 1 (next page) contains descriptions of the contents of each lane in Figure 8. The sample in Lane 1 was taken from the bacterial lysate and contains high protein content, as shown by the intense signal and lack of distinct protein bands. The samples used in Lane 2 and Lane 3 were taken during the later stages of ITC, with the sample in Lane 3 being taken after Lane 2. The protein content in Lane 2 appears to be similar to the protein found in Lane 1, indicating high protein content. In contrast, Lane 3 contains less protein than the bacterial lysate and Lane 2, and a single band between 15 kDa and 35 kDa is apparent. This demonstrates that ITC does remove impurities as the cycle progresses. Lane 4 contains the lyophilized EGF-ELP. The protein sample at this stage has been through the entire ITC process, dialyzed for 18 hours, and lyophilized.

Lane 4 contains a single band at approximately 30 kDa, demonstrating it is possible to successfully remove impurities while purifying the EGF-ELP using ITC.

Table 1 Lane descriptions for Figure 8

Lane	Description
L	Biotin Ladder
1	Bacterial Lysate
2	Cold Supernatant
3	Hot Pellet
4	Lyophilized EGF-ELP

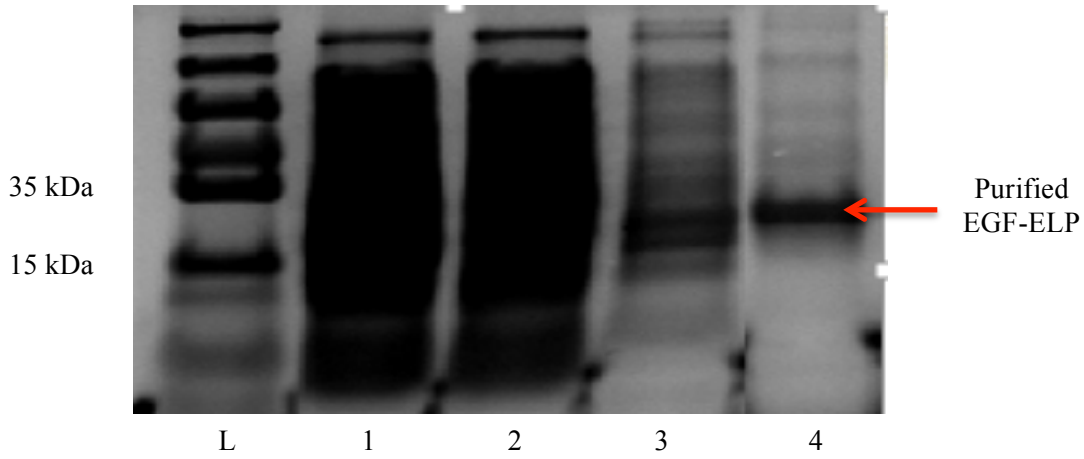

Figure 8 ITC is able to remove impurities from bacterial lysate. Samples from various stages of ITC were separated via gel electrophoresis on a 12% SDS-PAGE gel.

To confirm EGF-ELP was the protein isolated during ITC, samples from several stages of ITC were taken and underwent western blot analysis using anti-EGF. Figure 9 (next page) provides information pertaining to the ability of the EGF-ELP to be purified efficiently via ITC, and Table 2 (next page) provides information regarding the contents of each sample. The protein bands near 30 kDa indicate the presence of EGF-ELP (MW=26.7 kDa). Figure 9 shows the EGF-ELP is present in the bacterial lysate after sonication. The western blot also shows the EGF-ELP did not solubilize completely as it is present in the cold pellet (Lane 2) and cold supernatant

(Lane 3) in roughly equal amounts after the first cold centrifugation. Additionally, the protein bands present in the hot pellet (Lane 4) and hot supernatant (Lane 5) indicate the EGF-ELP is present in both samples after the first hot centrifugation. However, the signal in the hot pellet is more intense than the signal in the hot supernatant, indicating there is a larger quantity of the EGF-ELP in the hot pellet. Finally, the band seen in the lyophilized product demonstrates the final product contains the EGF-ELP (Lane 6), and the minimal background noise indicates there are relatively few impurities present in the lyophilized EGF-ELP product.

Table 2 Lane descriptions for Figure 9

Lane	Description
L	Biotin Ladder
1	Bacterial Lysate
2	Cold Pellet
3	Cold Supernatant
4	Hot Pellet
5	Hot Supernatant
6	Lyophilized EGF-ELP

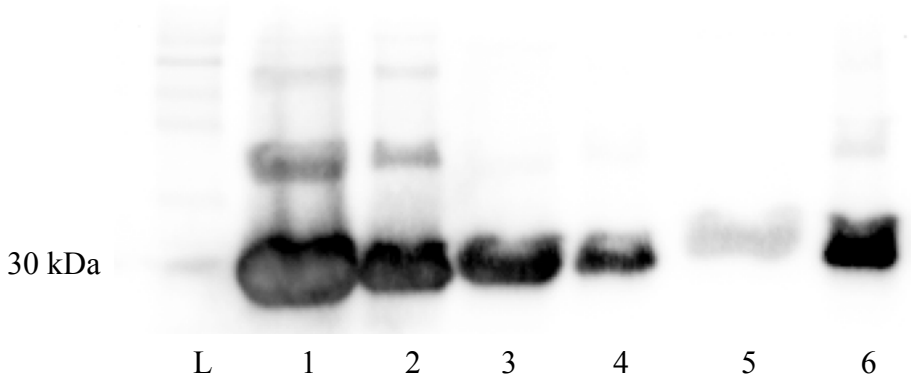

Figure 9 EGF-ELP can be purified via ITC. Samples form various stages of ITC were collected and subjected to western blot analysis to detect the presence of EGF-ELP.

2.4.2 EGF-ELP Transitions Below Physiological Temperature

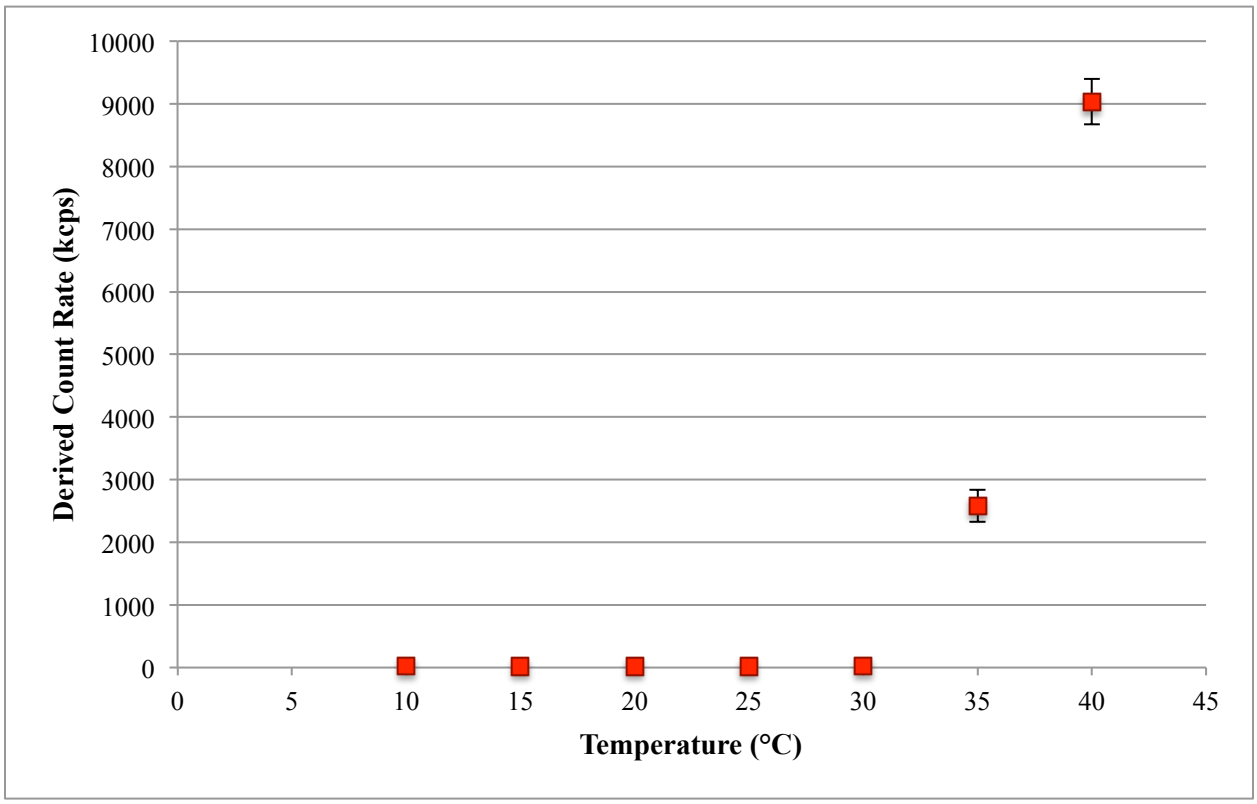

Figure 10 EGF-ELP transition temperature. Dynamic light scattering (DLS) was used to measure the mean count rate at temperatures in intervals of 5°C between 5°C-40°C. A 25 μM sample of EGF-ELP was used.

The transition temperature of the EGF-ELP was determined using dynamic light scattering (DLS). The mean count rate of a 25 μM sample was recorded over a temperature range of 10°C-40°C in 5°C intervals, and plotted in Figure 10 (above). An increase in derived count rate corresponds to the transition of EGF-ELP from monomers to aggregates. From 10°C-25°C, the mean count rate stays fairly constant at approximately 200 kilocounts per second (kcps). Once the temperature reached 30°C, the mean count rate increased from 200 kcps to 850 kcps, indicating the aggregation of EGF-ELP's. The transition temperature likely lies between 30°C-35°C. As the temperature was increased further to 35°C and 40°C the mean count rate increased

to 1250 kcps and 2600 kcps, respectively. The continued increase in mean count rate denotes a further increase in EGF-ELP aggregate size.

2.4.3 EGF-ELP Retains Elasticity of ELPs

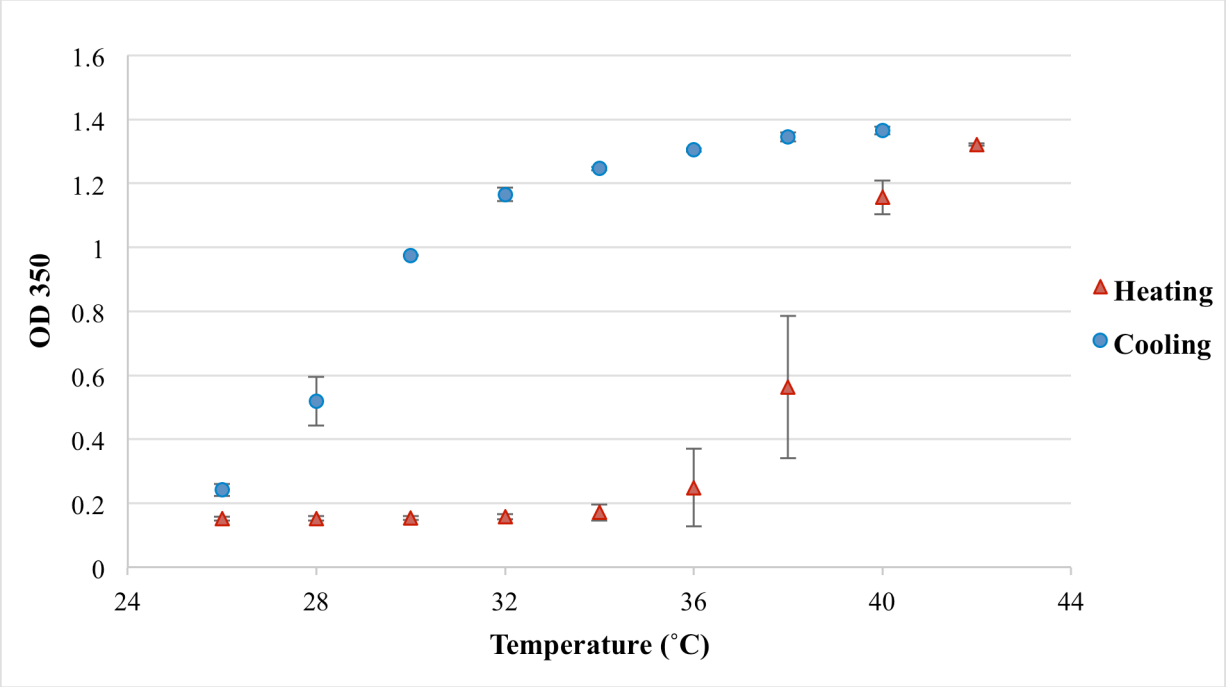

Figure 11 Thermoresponsive behavior of EGF-ELP. The OD 350 was measured while increasing the temperature from 26°C-42°C and while decreasing the temperature from 42°C-26°C.

Figure 11 (above) shows the optical density at 350 nm (OD 350) for a 15 μM solution of EGF-ELP. The OD 350 was measured as the EGF-ELP solution was heated from 26°C-42°C and then cooled from 42°C-26°C in increments of 2°C. As the sample was heated from 26°C-42°C, the OD350 value increased from 0.152 (+/- 0.006) to 1.322 (+/- 0.004), indicating the formation of EGF-ELP aggregates. Though, the OD 350 value did not increase significantly until the sample was heated to 38°C. When the solution was cooled from 42°C to 26°C, the OD 350 value decreased from 1.322 (+/- 0.004) to 0.241 (+/- 0.018), showing the EGF-ELP was able to be

solubilized after forming aggregates. Although, there was not a noticeable difference in the OD 350 value until the temperature was decreased to 36°C.

2.4.4 EGF-ELP Partially Solubilizes When Below T_t

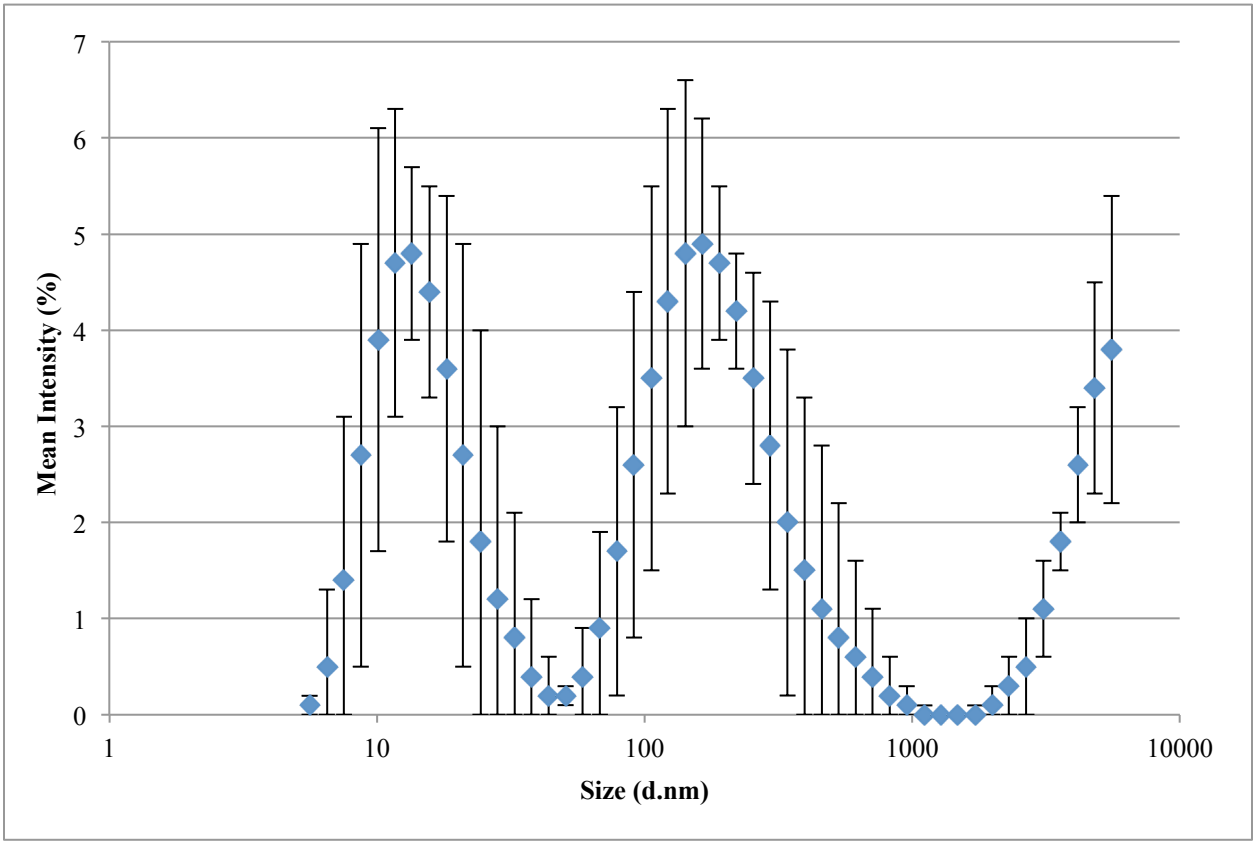

Figure 12 EGF-ELP particle size distribution at 4°C. EGF-ELP was diluted in PBS to a concentration of 5 μM and analyzed at 4°C using DLS. Particle size distribution is represented as mean intensity (%).

Further data relating to EGF-ELP thermoresponsive behavior was obtained using dynamic light scattering (DLS). DLS was conducted below the transition temperature (4°C) and above the transition temperature (37°C) to determine the size of EGF-ELP monomers and aggregates, and determine the particle size distribution. 3 measurements were recorded at each temperature. At 4°C, the Z-average value of the EGF-ELP was 61.00 nm with an average PDI value of 0.377 (data not shown).

Figure 12 (previous page) contains DLS data comparing the mean intensity as a function of EGF-ELP particle size. From Figure 12, it can be concluded that the particle size distribution is multimodal, with an approximate range of 5.61 nm-5560 nm. Relative maxima for mean intensity are found at 11.7 nm (4.7%) and 5560 nm (3.8%) with an absolute maximum at 142 nm (4.9%)

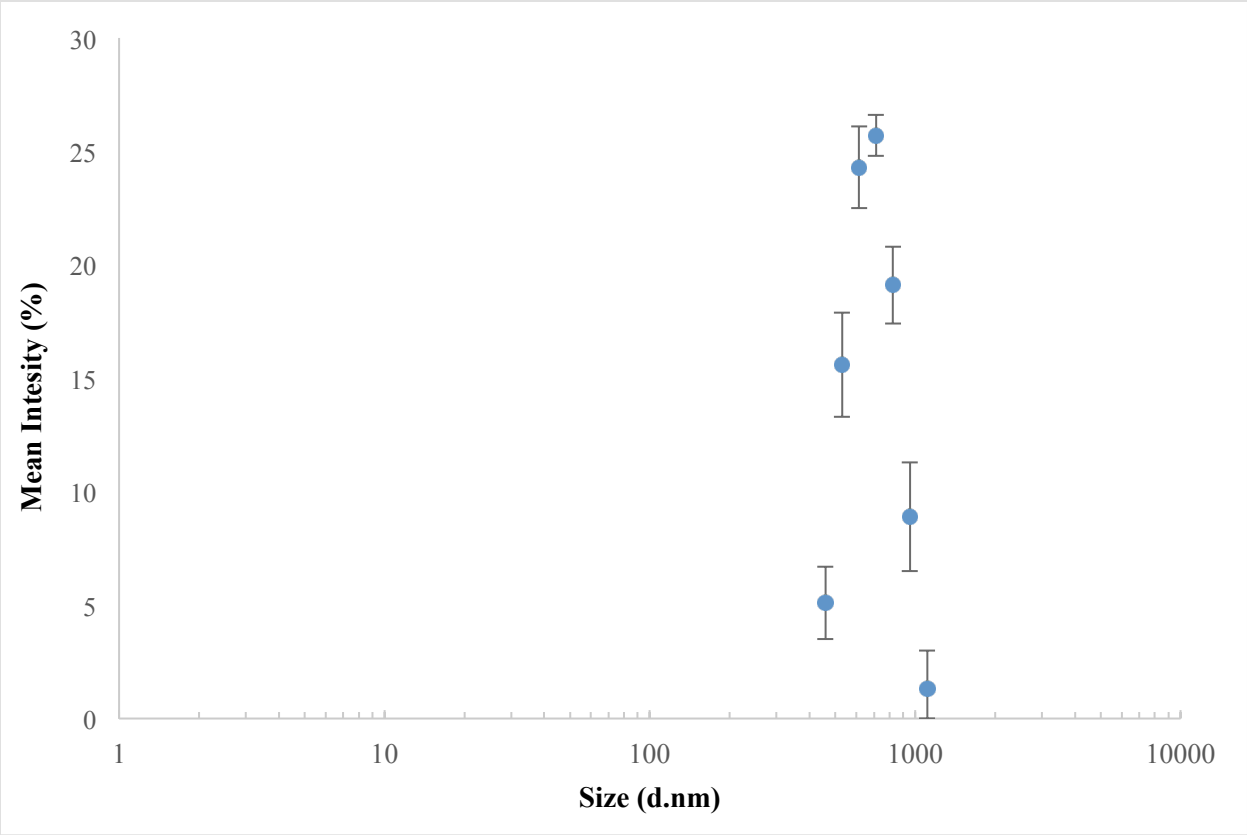

Figure 13 EGF-ELP particle size distribution at 37°C. EGF-ELP was diluted in PBS to a concentration of 5 μM and analyzed at 37°C using DLS. Particle size distribution is represented as mean intensity (%).

When DLS was conducted at 37°C, the Z-average of the EGF-ELP aggregates was determined to be 684.15 nm with an average PDI of 0.055 (data not shown). The relatively low PDI value indicates the Z-average value is reliable and that the data is monodispersed. Figure 13 (above) provides data relating the % intensity and particle sizes. Figure 13 shows the particle size distribution is monomodal and monodispersed, with a range of approximately 459 nm-1100 nm.

The maximum mean intensity value was found to occur at 712 nm with a mean intensity value of 25.7%.

2.4.5 EGF-ELP Induces Proliferation of A549 Cells

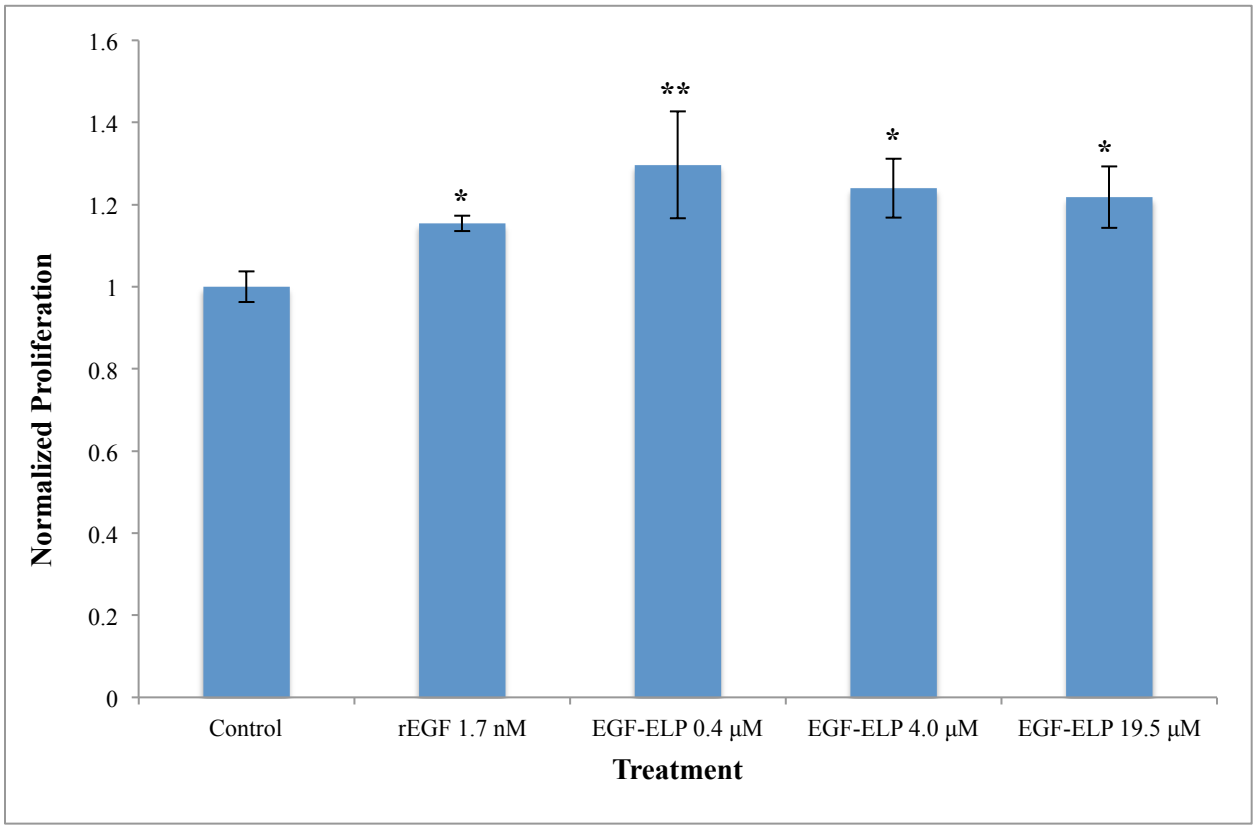

Figure 14 Induced A549 cell proliferation using EGF-ELP. A549 cells were treated for 48 with the described concentration of rEGF or EGF-ELP. Cell proliferation was quantified using a BrdU assay. For statistical significance, * = $p \leq 0.05$ and ** = $p \leq 0.10$.

Recombinant EGF (rEGF) has been shown to induce proliferation of non-small cell lung cancer (NSCLC) cell lines, such as A549 adenocarcinomic epithelial cells. NSCLC cell lines overexpress the EGFR, making them ideal to test the biological activity of the EGF-ELP [39]. Cell proliferation was measured using a bromodeoxyuridine (BrdU) assay to quantify the synthesis of new DNA after 48 hours of treatment. The results in Figure 14 (above) show the EGF-ELP retained the biological activity of rEGF by increasing cellular proliferation nearly 20% when compared to the control after 48 hours of treatment for all 3 concentrations used.

2.4.6 EGF-ELP Induces Migration of A549 Cells

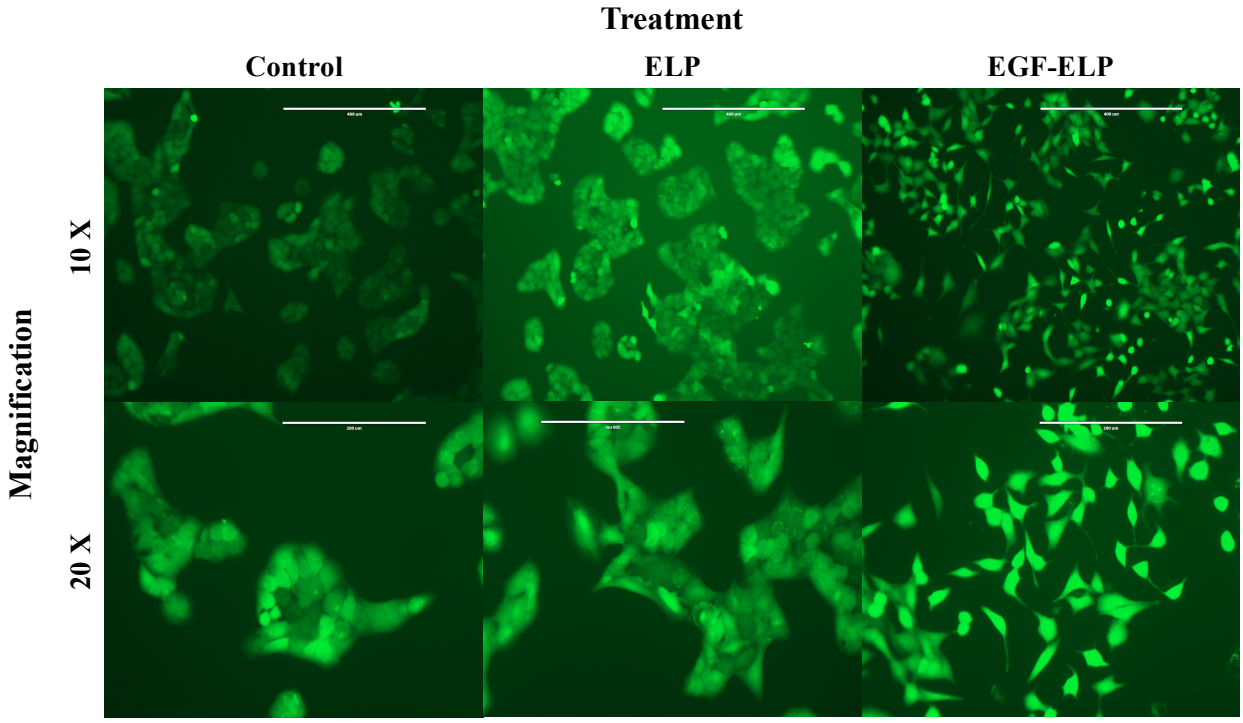

Figure 15 EGF-ELP induced A549 migration. A549 cells were treated with ELP or EGF-ELP (5 μM) for 48 hours, after which cells were stained with calcein to aid in visualization of cell morphology and migration.

EGF has also been shown to induce the migration of A549 cells [40]. To further investigate the biological activity of the EGF-ELP, A549 cells were treated with serum free media as a control, ELP or EGF-ELP (5 μM) for 48 hours, after which they were stained with calcein and photographed to observe differences in migration patterns. Figure 15 (above) shows the results. Treatment with ELP did not produce any change in cell or cell colony morphology when compared to the control group, with both forming tightly packed colonies. Treatment with EGF-ELP induced a change in cell morphology compared to the control and ELP treatment. A549 cells treated with EGF-ELP appear to have an elongated morphology and do not form distinct colonies as the control and ELP treated cells do.

2.4.7 EGF-ELP Inhibits Proliferation of A431 Cells

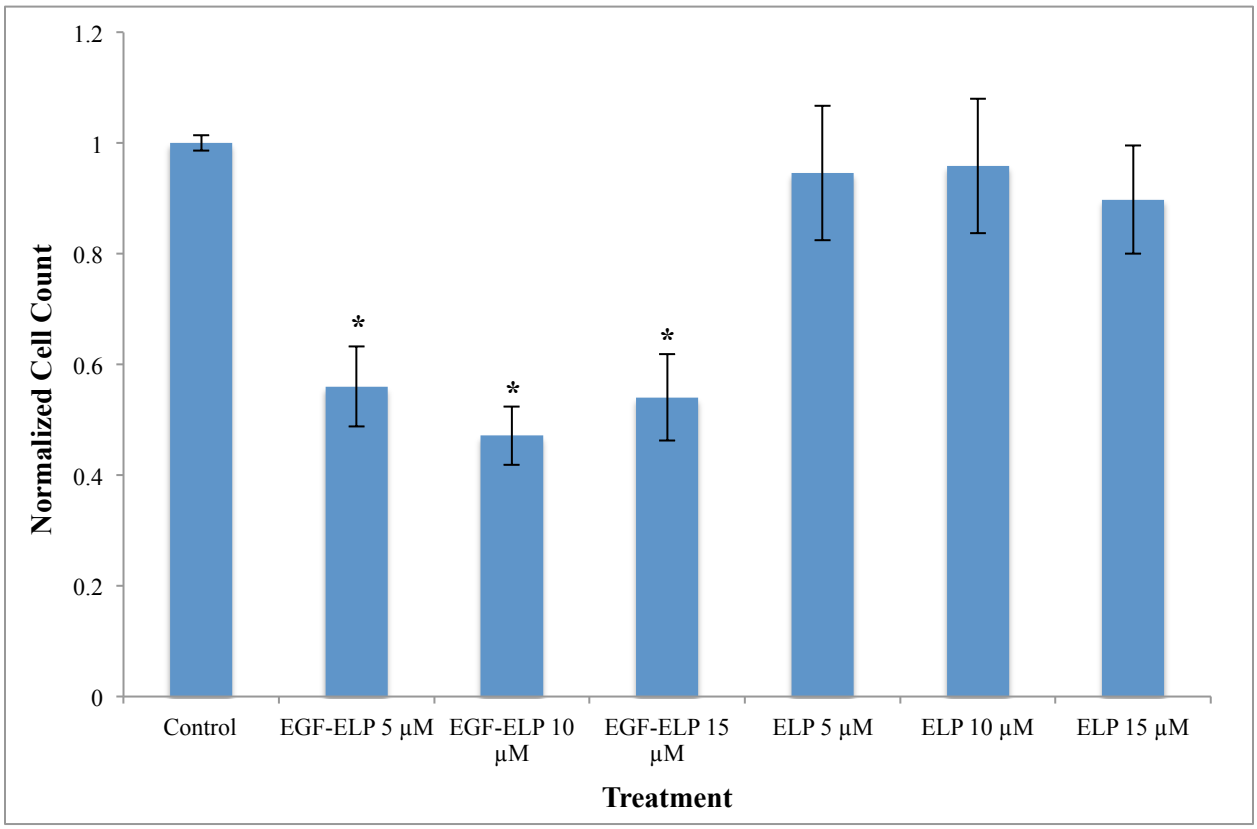

Figure 16 Inhibition of A431 cellular proliferation with EGF-ELP. A431 cells were treated with various amounts of EGF-ELP and ELP for 48 hours. Cells nuclei were stained with NucBlue and dead cell nuclei were stained with ethidium homodimer, and then counted using an ImageJ macro.

It has been demonstrated that EGF is able to inhibit cell proliferation of certain cells overexpressing the EGFR, such as A431 epidermoid carcinoma cells [41]. To determine whether the EGF-ELP was biologically active, A431 cells were treated with various concentrations of ELP or EGF-ELP for 48 hours, after which the number of live cells was counted. Figure 16 (above) shows the results of the biological activity assay after being normalized to the untreated control. When A431 cells were treated with EGF-ELP (5 µM, 10µM, and 15 µM), the number of live cells counted decreased by nearly 50% when compared to the untreated control and the ELP

controls. ELP controls did not experience a statistically significant increase or decrease in cell count after 48 hours of treatment when compared to the untreated control.

2.4.8 Induction of Human Skin Fibroblast Proliferation Using EGF-ELP

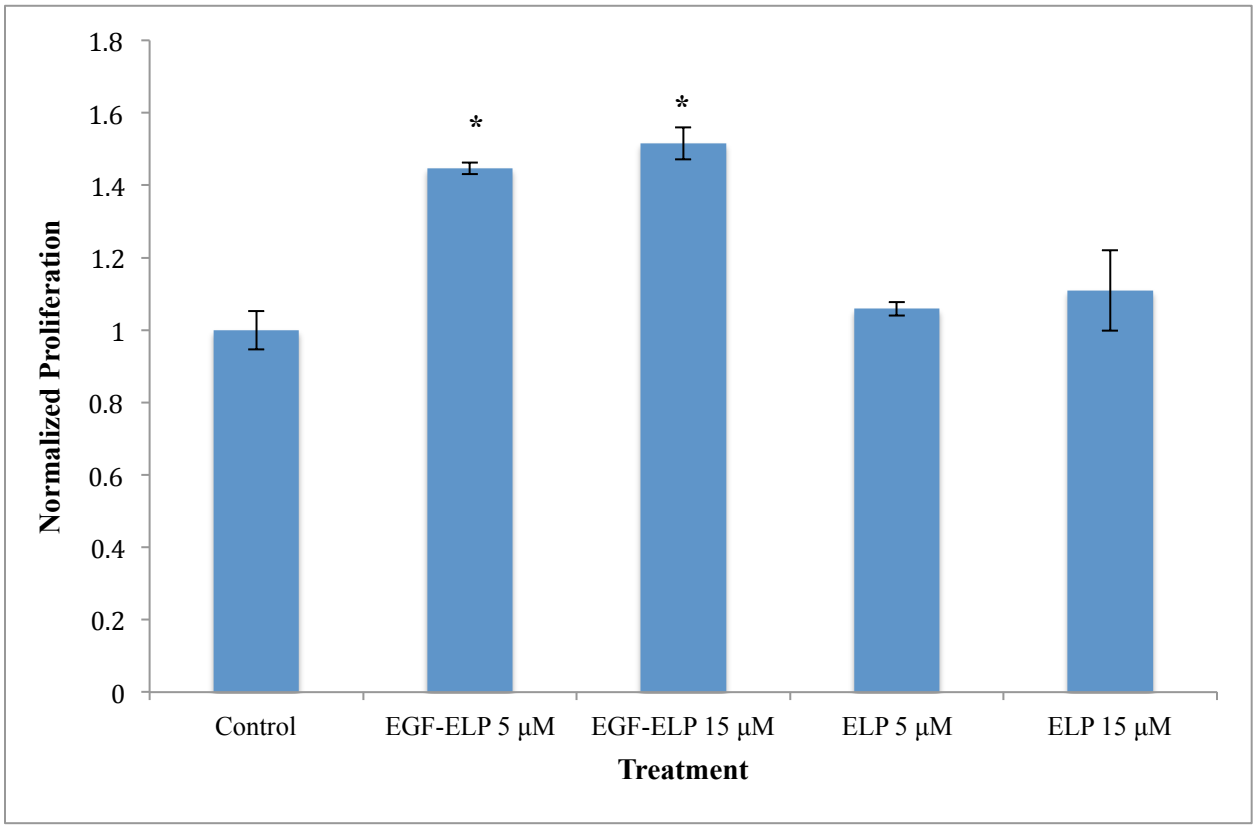

Figure 17 Proliferation of human skin fibroblast using EGF-ELP. Fibroblasts were treated for 48 hours in serum-free media, after which a Hoescht assay was conducted to determine cell proliferation. * denotes a p value ≤ 0.05.

EGF has been shown to promote cellular proliferation in human fibroblast [42, 43]. So to further test the biological activity of the EGF-ELP, human skin fibroblasts were treated with EGF-ELP for 48 hours and a Hoescht assay was performed to determine cell proliferation. The data (Figure 17, above) shows that the EGF-ELP does induce proliferation of human skin fibroblasts when compared to serum-free controls and ELP controls. Both EGF-ELP treatments, 5 µM and 15 µM, caused an approximately 45% increase in cell proliferation. ELP treatments did not cause any statistically significant increase in fibroblast proliferation.

2.5 Discussion

The aim of this study was to create an EGF-ELP fusion protein that could be used for regenerative medicine applications. Exogenous EGF has been used in regenerative medicine with moderate success to treat acute wounds, but minimal success has been seen in chronic wounds. This has been attributed to the harsh microenvironment in chronic wounds, which leads to enhanced degradation of exogenous growth factors [30, 31]. Additionally, EGF is typically administered in a bolus solution, which allows EGF to easily diffuse away from the injection site. Both increased degradation and diffusion lead to poor bioavailability of the growth factor; hence, minimal improvements are seen with EGF administration in chronic wounds [32].

The EGF-ELP fusion protein we have fabricated may assists in overcoming these hurdles in EGF administration. To start, the ability to undergo self-assembly at physiological temperature may allow for the formation of drug depots at the injection site, increasing the local concentration of EGF and possibly limiting diffusion of EGF. In addition, the EGF-ELP fusion protein can be used to create EGF-ELP infused hydrogels, similar to fibrin hydrogels infused with KGF-ELP fusion protein [18]. The ELP domain of the EGF-ELP could also be crosslinked with a scaffold to immobilize EGF, thereby creating a concentration gradient promoting cell migration and proliferation into the scaffold which could further aid tissue regeneration [38]. Another benefit of the EGF-ELP fusion protein is the drug and drug carrier are one and produced as one by bacteria, removing the need to physically or chemically conjugate EGF with a delivery vehicle.

The biological activity assays using human skin fibroblasts, A549 cancer cells, and A431 cancer cells all show the EGF-ELP retains the biological activity of EGF. In particular, the proliferation of fibroblast and induced migration of A549 cells demonstrates the potential for the

EGF-ELP to be used for wound regeneration as fibroblast and epithelial cell proliferation and migration are important components of the wound healing process, such as granulation tissue formation and epithelialization [44-46]. Although, the treatments did not appear to show any dose dependence. This is likely due to a dose threshold being reached using EGF-ELP. Future studies will use lower concentrations of EGF-ELP to determine the most effective concentration. Additionally, further experiments will be necessary to compare the regenerative capabilities of the EGF-ELP and rEGF. The migration of A549 cells will also need to be quantified to ensure the images are showing enhanced migration of A549 cells treated with EGF-ELP.

In addition to possessing the biological activity of EGF, the EGF-ELP retained the ability to undergo inverse phase transition, though the phase transitioning may have been impeded by the addition of EGF to the ELP. The OD350 data shows that the EGF-ELP fully retains the inverse phase transition property the ELP [47]. However, DLS data and the western blot show the fusion protein is not completely soluble. It is clear to see in the western blot that the fusion protein was not able to completely solubilize during ITC. The DLS data supports this further as shown by the presence of aggregates when the EGF-ELP solution was below the transition temperature (4°C). This may be the result of cysteine bonds forming between the EGF and ELP portions of the fusion protein rendering it less soluble, though this is unlikely due to the EGF-ELP retaining the biological activity of EGF [22]. This could also be caused by the relative hydrophobicity of EGF when compared to the ELP. The discrepancy between the OD350 and DLS data could be attributed to the increased sensitivity of DLS apparatus when compared to the spectrophotometer.

Even though the fusion protein was not able to completely solubilize, the EGF-ELP was purified via ITC. This could provide a relatively simple and inexpensive purification technique

for recombinant EGF when compared to affinity chromatography methods. Furthermore, it was found that by adding a hydrophilic FLAG-tag to the C-terminus of the fusion protein, EGF-ELP yields increased up to 3 times (data not shown). Size data for the FLAG-tagged ELP was obtained using DLS, (Appendix B). Further analysis will be conducted to determine the effect the FLAG-tag has on EGF-ELP biological activity.

Hence, we were able to develop a fusion protein that retained the biological activity of EGF and the inverse phase transition behavior of ELPs. Since the fusion protein was able to at least partially retain inverse transition properties, purification can be carried out using a simple ITC protocol. As demonstrated by biological activity assays, the EGF-ELP fusion protein has the potential to be used in the treatment of chronic wounds. In regenerative medicine applications the EGF-ELP could be used to increase the bioavailability of EGF via drug depot formation or conjugation to a scaffold. Treatment may be further enhanced if combined with other therapeutic ELP fusion proteins.

CHAPTER 3: DEVELOPMENT OF ELASTIN LIKE POLYPEPTIDE BASED HYDROGEL USING PHOTOREACTIVE AMINO ACID ANALOGS

3.1 Introduction

The regeneration of lost tissue function is one of the biggest challenges facing clinicians and researchers, currently. The loss of tissue function can be the result of several types of occurrences, including trauma, degenerative disease, congenital disease, or oncologic resections [48, 49]. The treatment of these injuries is traditionally conducted using allografts [50], xenografts [51], tissue/organ transplants [52], or synthetic biomaterials that replace the lost tissue [53]; however, these approaches do not always produce adequate results. The prominence of poor outcomes can be attributed to a variety of factors such as immune rejection, the need for patients to undergo complex surgical procedures, and tissue/organ donor shortages [54, 55]. Hence, novel approaches have been investigated to aid in the restoration of lost tissue function.

One approach that has shown great potential in the restoration of lost tissue function is the combined use of growth factors, cells, and biomaterials to replicate a microenvironment that promotes tissue regeneration [56, 57]. Though, this approach presents its own obstacles that must be overcome. Two of the main factors limiting the utilization of this approach are the short half-life and limited bioavailability of exogenous growth factors [58]. The importance of biomaterials becomes apparent when considering these problems, as demonstrated by the fact that many new growth factor delivery systems utilize biomaterials for drug delivery. The main advantage provided by biomaterials is the ability to physically encapsulate growth factors within the material, which protects growth factors from degradation at the injury site. Biomaterials also

assist in maintaining sufficient growth factor concentrations at the injury site by providing a means of localized delivery and reducing diffusion away from the wound site. This removes the need to continuously reapply growth factors during therapy, decreasing costs and reducing the risk of adverse effects due to supraphysiological concentrations of growth factors. Furthermore, biomaterials can also function as structural scaffolds for host cell migration, further enhancing tissue regeneration [33].

3.1.1 Synthetic Biomaterials Used For Regenerative Medicine

There are a number of synthetic materials used for the delivery of growth factors. Some of the more traditional synthetics are poly-lactic acid (PLA) [59], polyglycolic acid (PGA) [60], polyethylene glycol (PEG) [61], and copolymers such as polylactic-co-glycolic acid (PLGA) [62]. The primary benefit of using synthetic materials is the ability to manipulate the material properties based on the clinical application. For example, certain applications, such as bone and cartilage engineering, require the construction of scaffolds that will retain their physical and chemical properties over a significant period of time; hence, a nonbiodegradable polymer, such as PEG, can be used [61, 63]. Different applications may require the scaffold to degrade at the same rate as tissue regeneration. In these instances, biodegradable synthetic materials such as PLA [59] or PGA [60] can be used to construct the scaffold.

While synthetic materials are highly tunable making them suitable for various applications, there are drawbacks. One of the major limitations is the inherent lack of intrinsic biological activity in synthetic materials, such as cell adhesion, migration, and cell mediated degradation [64]. Thus, to surmount these issues synthetic materials have been functionalized with various biologically active groups such as heparin to improve growth factor loading [65], or RGD sequences to improve cell adhesion on PEG scaffolds [61]. However, the addition of

biologically active moieties requires chemical conjugation to the scaffold, which adds another step and time to scaffold construction. Furthermore, special considerations must be taken when using synthetic materials because they, or their degradation products, may be toxic or difficult to remove from the body [33].

3.1.2 Naturally Derived Biomaterials Used for Regenerative Medicine

In addition to synthetic materials, naturally derived biomaterials such as collagen [66], gelatin [67], chitosan [68], fibrin [69], and elastin [70] have also been utilized for growth factor delivery in regenerative medicine. The use of naturally derived materials provides many benefits for regenerative therapy. For one, natural materials minimize inflammation associated with the implantation of biomaterials because of their natural origin. Also, many naturally derived biomaterials possess intrinsic biological activity that supports tissue regeneration, further enhancing the regenerative capability of the delivery system. Lastly, since most naturally based materials are soluble in water, their fabrication can be carried out under conditions that do not alter the biological activity of the biomaterial or associated growth factors [33].

When used in combination with natural materials, growth factors are typically infused into the scaffold or dispersed within the biomaterial before scaffold polymerization. The release of growth factor is then determined by the scaffold's degradation rate and the rate of growth factor diffusion out of the scaffold. This can present a problem because it can be difficult to control the rate of scaffold degradation and since growth factors are not conjugated to the biomaterial itself, growth factors can readily diffuse out of the scaffold leading to burst release profiles [33]. To gain control over growth factor release profiles, modifications to the biomaterial can be made so that growth factors can bind to the biomaterial more effectively, similar to approaches taken using synthetic materials. For instance, EGF infused hydrogels have been used

for corneal epithelial wound healing. However, it was found that when cationized gelatin hydrogels were used, the interaction between the cationized gelatin and EGF allowed for increased control over EGF release. The increased control over the EGF release profile resulted in improved corneal wound healing [26]. Additionally, heparinized chitosan has been used to bind FGF and better control FGF release from chitosan scaffolds [71].

3.1.3 Elastin Like Polypeptides in Regenerative Medicine

As mentioned in Chapter 1, ELPs are a class of genetically encodable, nonimmunogenic, biodegradable polymeric proteins. The amino acid sequence consists of the pentapeptide repeat $(VPGXG)_n$ where X is any guest residue other than proline and n is the number of pentapeptide repeats. Since ELPs are genetically encodable, it is possible to encode biologically active molecules into an ELP sequence, creating biologically active ELP fusion proteins. ELPs also have the ability to undergo inverse phase transitioning near physiological temperatures. When below their inverse phase transition temperature (T_t), ELPs are soluble in aqueous solution. Although, when above their T_t ELPs undergo self-assembly, making them insoluble in aqueous solution. This property is conserved in ELP fusion proteins, providing means of purification for ELPs and ELP fusion proteins via inverse transition cycling (ITC) [2].

The ability to self-assemble also enables ELPs to form nanoparticles and coacervates. Hence, ELPs can be applied to injury sites to serve as not only drug depots, but as drug delivery vehicles for biologically active moieties. Additionally, physiosorption or chemical conjugation of peptide sequences to ELPs is not required since they are genetically encodable, making synthesis of the drug and drug delivery vehicle a single step. The physical properties of ELPs can also be fine-tuned by making alterations to ELP chain length and guest residue identity. For instance, ELPs that form micelles have been designed using block copolymers. Moreover, ELP sequences

have been constructed that allows for the formation of hydrogels via physical or covalent crosslinking [2].

3.1.4 Hydrogels as Drug Delivery Vehicles in Regenerative Medicine

Hydrogels are three-dimensional networks composed of hydrophilic polymers that are covalently crosslinked to one another, or are held together through intramolecular and intermolecular physical interactions. Hydrogels are able to absorb large quantities of water and biological fluids without dissolving; hence, hydrogels are able to effectively encapsulate and release many important biomolecules, such as growth factors. Also, hydrogels are highly permeable to oxygen and nutrients, and can be engineered to allow cell adhesion and migration making them useful for tissue regeneration. Additionally, the high water content of hydrogels gives them mechanical properties similar to that of soft tissues. When combined, these properties make hydrogels remarkably attractive options for regenerative medicine applications [72]. Hydrogel formulations that can be injected in an aqueous form and then crosslinked *in situ* are especially useful because it allows the hydrogel to form to the shape of the defect, providing an improved fit at the wound site [33].

3.1.5 Hydrogels Through Physical Interactions

One of the many ways to categorize hydrogels is the method by which their polymer network is crosslinked. Physical crosslinking is a common method utilized for hydrogel formation and can be accomplished via ionic interaction, hydrogen bonding, and hydrophobic interactions [72]. Hydrogels prepared through ionic interactions are formed when charged sites on the polymer backbone interact and hold polymer chains together. This method has been used to synthesize chitosan-alginate hydrogels for the controlled delivery of ampicillin [73]. Hydrogels formed via hydrogen bonds are crosslinked by the interaction between electron

deficient hydrogen atoms (protons) and functional groups with high electronegativity. Hydrogen bonding has been used to produce poly(vinyl alcohol)/DNA hydrogels for gene therapy [74]. Lastly, to form hydrogels via hydrophobic interactions, polymer chains containing hydrophobic micro-domains are used. The hydrophobic portions of the polymer backbone act as the crosslinking domains for the hydrogel. ELP hydrogels have been synthesized using hydrophobic interactions between triblock polymers; though, as with many physically crosslinked hydrogels, the hydrogel did not possess sufficient mechanical strength [2, 75].

3.1.6 Covalent Binding of Hydrogels via Chemical Crosslinking

To improve the mechanical strength of ELP based hydrogel platforms, various covalent crosslinking methods of ELPs have been employed. McMillan and Conticello demonstrated that periodic lysine residues could be crosslinked using bis(sulfosuccinimidyl) suberate [19]. Numerous other crosslinking agents, such as tri-succinimidyl aminotriacetate [76], glutaraldehyde [77], transglutaminase [78], and genipin [79] have been used to covalently crosslink ELPs via lysine and glutamine residues, predominantly. Furthermore, [Tris(hydroxymethyl)phosphine]propionic acid[betaine] has been used to create injectable hydrogels composed of ELP polymers [80]. Even though the use of chemical crosslinking for hydrogel preparation has proven useful, there are disadvantages to this approach. The primary concern is the use of crosslinking agents themselves. These crosslinking agents are often nonspecific and require the use of toxic solvents that could negatively affect cell viability [81]. Additionally, hydrogel formation is initiated immediately after the addition of the crosslinker. This results in the formation of non-homogenous hydrogels, which may have significant impacts on tissue regeneration at the cellular level [82]. Figure 18 (next page) illustrates how covalent crosslinking of ELP monomers can be used to produce hydrogels.

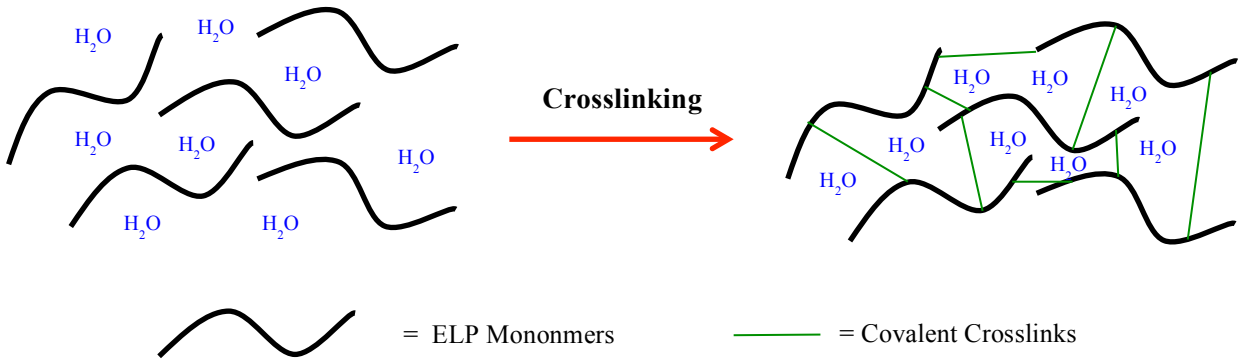

Figure 18 Covalent crosslinking for hydrogel formation. ELP monomers in aqueous solution can be covalently crosslinked creating a polymer network that can retain water.

3.1.7 Photocrosslinkable Polymers

Photocrosslinking can be utilized to combat many of the issues associated with physical and chemical crosslinking. Harnessing light as a crosslinking agent is an attractive option for several reason, including the rapid rate of reaction, low energy requirements, use of solvent free formulations, and low cost. In addition, focused light sources and photomasks can be used during photocrosslinking to provide spatial and temporal control [82]. As a result of these findings, polymers have been functionalized with photoreactive functional groups, such as methacrylate [83], diazirine [82], or aryl-azides [84] to create photocrosslinkable hydrogels. However, these platforms have one major drawback, the functionalization of the polymer backbone adds additional steps to the synthesis of the hydrogel. One step for the functionalization of the polymer, and another step for the removal of photoreactive groups that have not been incorporated. To remove the need for conjugation of photoreactive functional groups, photoreactive amino acid analogs have been utilized to create photoreactive recombinant proteins [20].

The use of photoreactive amino acid analogs provides many benefits over the conjugation of photoreactive moieties. To start, since recombinant proteins are genetically encodable, it is

possible to incorporate the photoreactive amino acid analogs at specific points in the protein sequence. Also, photoreactive amino acid analogs can be activated without the use of photoinitiator. Finally, photoreactive amino acids do not effect phase transition properties of ELPs, thus photoreactive polymers can be readily purified using ITC [20]. Photoreactive ELP based films have been described using *para*-azidophenylalanine (*p*N_3Phe) as a photoreactive amino acid analog. However, the incorporation of *p*N_3Phe into the ELP sequence required alterations to the bacterial translational machinery due to the difference in structure between *p*N_3Phe and naturally occurring phenylalanine [20].

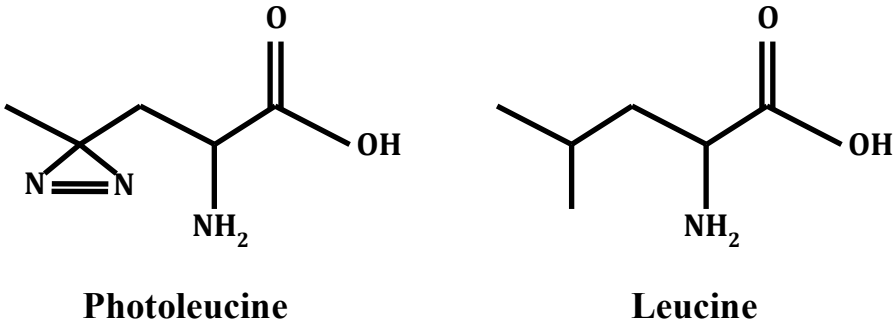

Figure 19 Structures of photoleucine and leucine. In photoleucine, a methyl group on the γ-carbon is replaced by a dizarine group.

A new class of photoreactive amino acid analogs has been developed to overcome the need for modification of bacterial translational machinery. This new class has photoreactive diazirine rings incorporated into the amino acid side chain, as shown in Figure 19 (above). Due to the similarity in structure between the naturally occurring amino acids and the photoreactive analogs, there is no need to modify the bacterial translational machinery for the analog to be incorporated into the protein sequence. Furthermore, the diazirine chemistry can readily activated using long wave ultraviolet (UV) light (330-370 nm) and the crosslinking reaction is noncytotoxic, meaning crosslinking can be conducted *in situ* [85]. To further improve

incorporation of photoreactive amino acids, auxotrophic bacteria can be used for protein expression.

3.1.8 Noncanonical Amino Acid Substitution

Protein polymers have been used to create a variety of functional biomaterials. However, the side chains of canonical amino acid residues they are composed of limit their functionality. To further expand the functionality of protein polymers, noncanonical amino acid analogues, such as photoreactive amino acids, have been incorporated into recombinant proteins [20]. To incorporate noncanonical amino acids, auxotrophic bacterial expression host are typically used [86]. In auxotrophic bacteria, genes for biosynthetic pathways that produce specific canonical amino acids have been knocked out, thereby reducing the bacteria's ability to produce certain amino acids. This is advantageous because if the auxotrophic bacteria are starved of the canonical amino acid for which they are auxotrophic, and a noncanonical analog of the amino acid is added to the expression media, there will be an increased rate of noncanonical amino acid incorporation; thereby allowing for increased functionalization of protein polymers.

The substitution of noncanonical amino acid analogs was originally limited to analogs with structural similarity to the canonical amino acids. Similarities in structure allow noncanonical amino acids to avoid the proofreading mechanisms in the translational machinery. However, the number of noncanonical amino acids available has been expanded to include analogs with dissimilar structures through the manipulation of protein expression host's biosynthetic machinery [86]. For instance, mutated amino-acyl tRNA synthetases have been introduced into *E. coli* that possess enlarged binding domains [87] or reduced editing activity [88] to improve the incorporation of noncanonical amino acids.

3.2 Project Objective

There have been a number of platforms developed that serve as drug carriers and structural scaffolds. However, these systems typically require either physiosorbtion or chemical conjugation of biologically active moieties and crosslinking domains to the scaffold, making their synthesis more complicated and time consuming. Additionally, many of these platforms use cytotoxic crosslinking agents, and cannot be injected into a defect in aqueous form and crosslinked *in situ,* providing a better fit at the defect site. The aim of this project was to develop a platform that not only serves as a drug delivery vehicle and structural scaffold, but also removes the need for conjugation of bioactive peptides and crosslinking motifs to the material, and is able to be crosslinked *in situ* after injection in an aqueous form. To achieve these goals, we set out to create a novel class of photocrosslinkable and biologically active ELPs that can be synthesized in a single step.

3.3 Materials and Methods

3.3.1 Materials

The monomeric gene fragment encoding $(VPGLG)_5(VPGVG)$ (referred to as L_5) was purchased from GenScript. Restriction enzymes and other enzymes used for cloning were purchased from New England Biolabs. For purification of DNA after gel electrophoresis, a gel extraction kit (Qiagen) was used. Naturally occurring amino acids and L-photoleucine were supplied by ThermoFisher Scientific. JW5807-2 leucine auxotrophic *Escherichia coli* developed by Baba et al were used for protein expression [89].

3.3.2 ELP Gene Construction

The ELP gene was constructed using a monomeric gene fragment encoding the L_5 ELP sequence. The monomeric gene fragment was excised from the pUC19 cloning plasmid using

*Pfl*MI and *Bgl*I restriction endonucleases, and the pUC19 cloning vector was linearized using *Bgl*I. Following gel electrophoresis and purification, the excised gene fragment underwent concatemerization to produce a gene encoding 3 monomeric gene fragment repeats. The newly synthesized gene was then ligated into the linearized L_5- pUC19 vector. This ligation produced a gene encoding L_{20}. The L_{20} pUC19 plasmid was then transformed into Top10*f* competent cells (Invitrogen). PCR was used to select bacterial colonies containing the L_{20} plasmid.

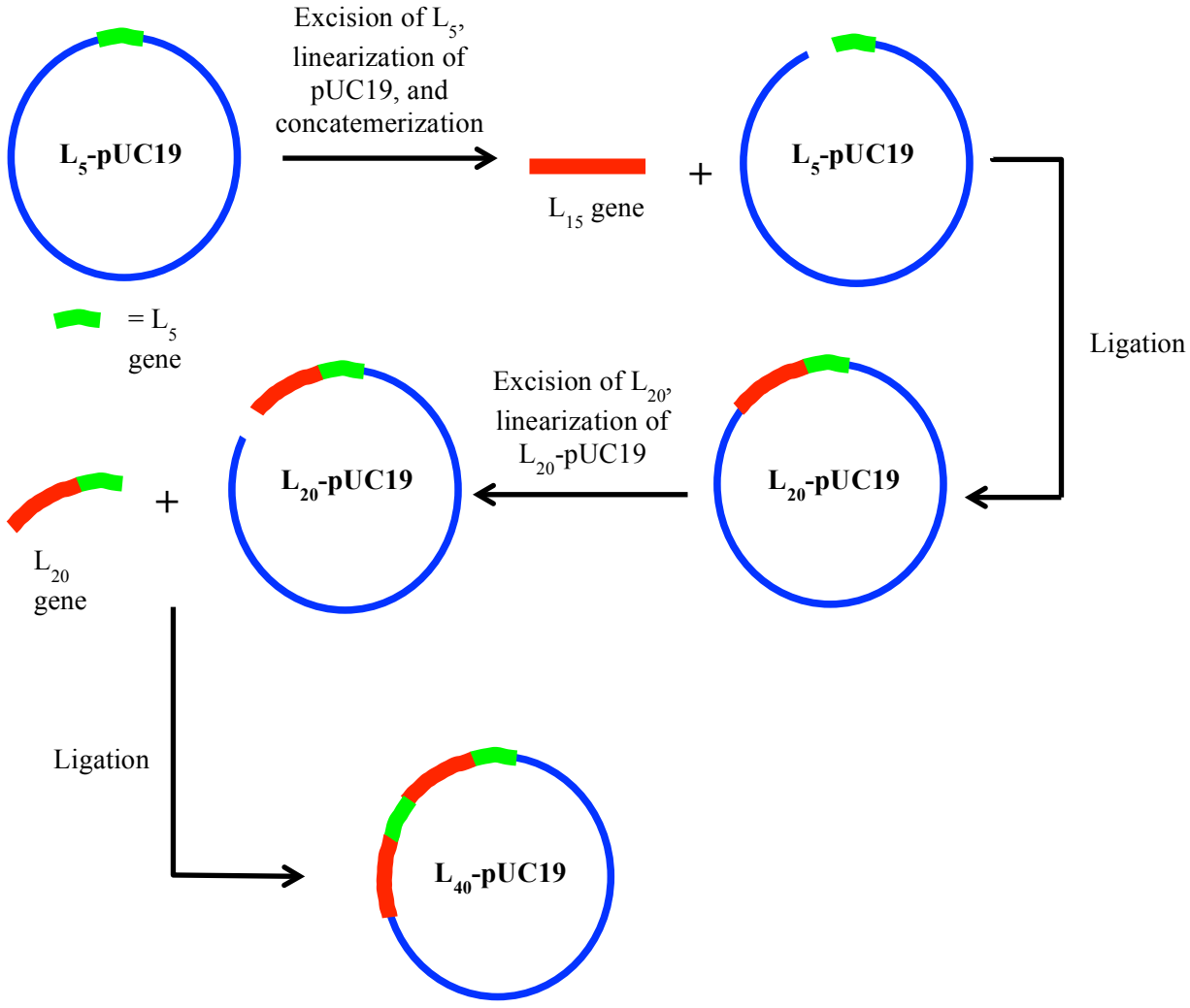

Figure 20 Construction of L_{40} (ELP) pUC19 cloning vector. The L_{40} gene was constructed from a L_5 monomeric gene fragment. The L_{40} gene was then excised and ligated into a linearized FLAG-pUC19 vector to create a L_{40}-FLAG gene, which was ligated into a pET25b(+) expression vector (not shown).

The L_{20} gene was then removed from the pUC19 plasmid using *Pfl*MI and *Bgl*I, and the L_{20} pUC19 plasmid was also linearized using *Bgl*I. After purification, the L_{20} gene was then ligated into the linearized L_{20}-pUC19 plasmid to produce a L_{40}-pUC 19 plasmid. The L_{40}-pUC19 plasmid was transformed into Top10*f* competent cells, and PCR was used to select for bacterial colonies containing the correct plasmid. Figure 20 (previous page) illustrates the cloning process up to this point. The L_{40} gene was then removed from the pUC19 cloning plasmid using *Pfl*MI and *Bgl*I, and purified. The L_{40} gene was then ligated into a linearized FLAG-pUC19 plasmid (FLAG-tag was placed at C-terminus of ELP) and transformed into Top10*f* competent cells. PCR was used to select bacterial colonies containing the appropriate plasmid.

The L_{40}-FLAG gene (ELP) was then removed from the pUC19 plasmid, purified, and ligated into a pET25b(+) expression plasmid linearized with *Sfi*I restriction endonuclease. Again, Top10*f* competent cells were used to transform the plasmid. Bacterial colonies underwent PCR and plasmids containing the L_{40}-FLAG gene were sent for DNA sequencing to ensure the correct gene was produced and that there were no genetic mutations. Once the DNA sequence was confirmed, L_{40}-FLAG pET25b(+) expression plasmids were transformed into JW5807-2 leucine auxotrophic *E. coli* for ELP expression.

3.3.3 Photoreactive ELP Expression

Leucine auxotrophic *E. coli* transformed with the pET25b(+) expression system containing the ELP gene were used to produce ELPs. Due to the inability of the bacteria to grow in standard M9 minimal media (Na_2HPO_4: 6 g/L , KH_2PO_4: 3 g/L, NaCl: 0.5 g/L, NH_4Cl: 1 g/L, $MgSO_4$: 1 mM, $CaCl_2$: 100 μM, glycerol: 0.2%, and carbenicillin: 100 μg/ml), a starter culture of TB media (no glycerol) containing 1% glucose as a carbon source was used as a starter culture for bacteria. The presence of 1% glucose as a carbon source prevented activation of the

pET25b(+) expression system containing the ELP gene. Inhibition of ELP expression is necessary until photoleucine has been added to media to maximize photoleucine incorporation.

Following overnight inoculation of bacteria in TB media, the overnight culture was added directly to standard M9 minimal media containing 1% glucose (1 ml TB culture : 20 ml fresh M9) until the culture reached an OD600 value of 0.7. Once the desired OD600 value was reached, the bacteria was centrifuged and washed in PBS to remove excess TB media. Bacteria were centrifuged again and resuspended in M9 minimal media containing the appropriate amount of supplemental amino acids, photoleucine, and isopropyl β-D-1-thiogalactopyranoside (IPTG) (1 mM) for ELP expression. Induction of ELP expression with IPTG lasted for 6-24 hours. The ELP expression protocol is described in Figure 21 (below).

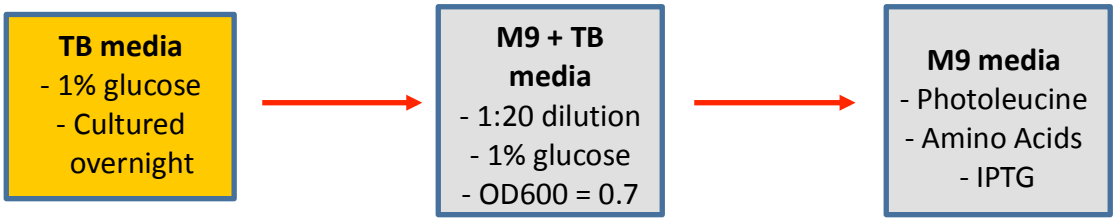

Figure 21 Photoreactive ELP expression. Leucine auxotrophic expression host were originally cultured in TB media containing 1% glucose, then transferred to fresh M9 media containing 1% glucose (1 ml TB: 19 mL M9) until sufficient levels of bacterial growth had been attained. Bacteria were then washed and resuspended in fresh M9 media supplemented with amino acids and IPTG to induce ELP expression.

3.3.4 *In vivo* Photocrosslinking

Photocrosslinking was conducted using a Blak-Ray® B-100AP/R High Intensity UV Lamp (365 nm, 100 watt, 60 Hz). Following induction of ELP expression, expression host were centrifuged and resuspended in 3 mL of 1x PBS. Bacteria suspension was placed in a 6 well tissue culture plate and exposed to UV light for 5 minutes. Following UV exposure, bacteria was centrifuged and lysed. The mechanism for photocrosslinking is illustrated in Figure 22 (next page).

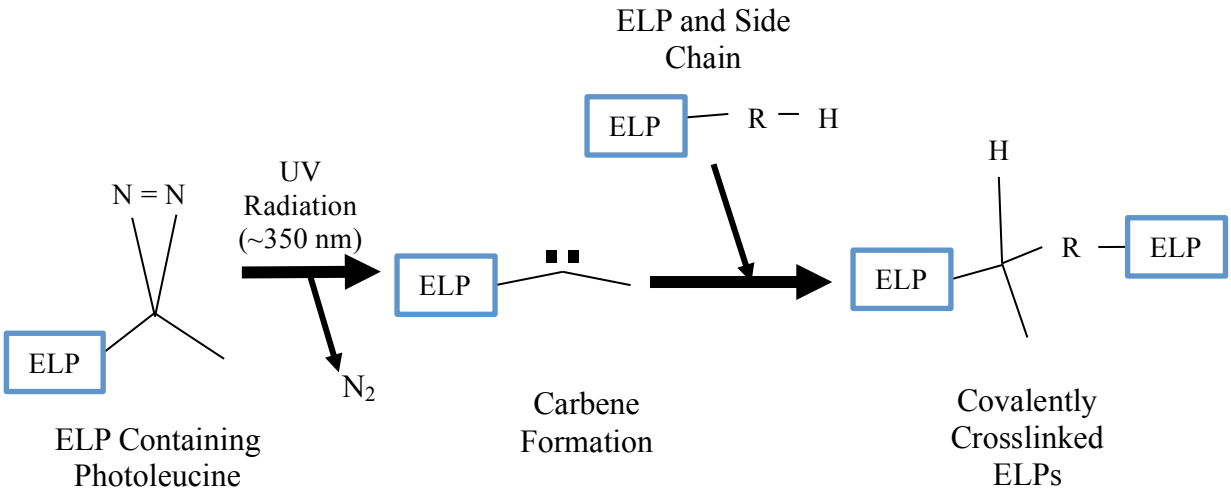

Figure 22 Photocrosslinking mechanism using photoleucine. UV radiation (~350 nm) causes carbene formation on photoleucine side chains. Carbene can react with any nearby amino acid side chains forming covalent crosslinks with ELP monomers.

3.3.5 Western Blot Analysis

Bacterial lysates were prepared and underwent SDS-PAGE analysis (12 % acrylamide). ELPs were labeled with anti-FLAG antibody (Sigma Aldrich), which was labeled using horseradish peroxidase (HRP) linked anti-rabbit secondary antibody (Cell Signal). A chemiluminescent signal to identify HRP-linked anti-rabbit was produced using LumiGLO Reagent and peroxide (Cell Signal).

3.4 Results

3.4.1 Inhibition of pET25b(+) Expression System Using 1% Glucose

To determine whether glucose was able to effectively suppress the pET25b(+) expression system used for ELP production, *E. coli* containing the FLAG-tagged ELP gene within the pET expression system was cultured for 24 hours in TB media with either 1% glucose or 1% glycerol used as a carbon source. Figure 23 (next page) depicts the results of SDS-PAGE analysis and Table 3 (next page) describes carbon source used for expression media. The presence of a protein band near 25 kDa in Lane 2 indicates the ELP gene was expressed when 1 % glycerol was

utilized as a carbon source (molecular weight of-ELP=20.2 kDa). However, the absence of the same band in Lane 1 suggests the pET system was inhibited since the ELP was not expressed in the presence of 1% glucose.

Table 3 Lane descriptions for Figure 23

Lane	Description
L	Biotin ladder
1	1% glucose
2	1% glycerol

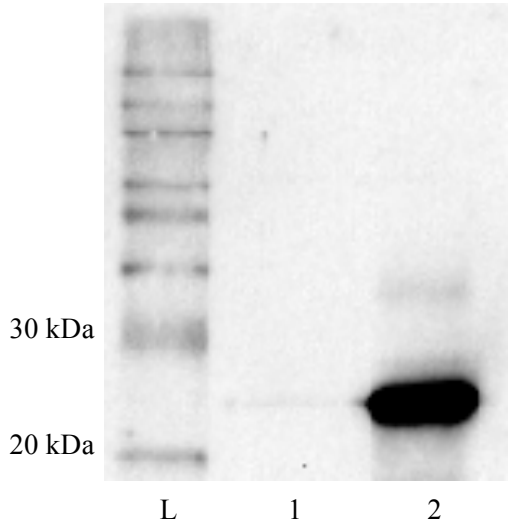

Figure 23 Glucose suppression of ELP expression. *E. coli* were cultured in TB media in the presence of 1% glucose or 1% glycerol. The presence of FLAG-tagged ELPs was detected via western blot analysis using anti-FLAG.

3.4.2 ELP Photocrosslinking *in vivo*

Figure 24 (next page) displays a western blot completed on bacterial lysates after exposure to UV radiation, while Table 4 (next page) describes the expression media conditions, and whether or not expression host were exposed to UV light. Leucine auxotrophic *E. coli* were cultured in M9 minimal media containing valine (1 mg/ml), proline (1 mg/ml), glycine (2 mg/ml), and either leucine (1 mg/ml) or photoleucine (1 mg/ml). Lanes 1-4 contain protein bands

at approximately 25 kDa, denoting the presence of ELP monomers that have not been photocrossinked. Though, Lane 1 contains an additional band at nearly 50 kDa indicating the presence of photocrosslinked ELP, possibly an ELP dimer. The increased signal in Lane 4 indicates elevated ELP expression levels when compared to Lane 2 and Lane 3. Due to the apparent crosslinking of ELP monomers in Lane 1, it is difficult to determine the relative amount of protein expression compared to other samples.

Table 4 Lane descriptions for Figure 24

Lane	Description
L	Biotin Ladder
1	p-Leu and UV
2	p-Leu and no UV
3	Leucine and UV
4	Valine, Proline, Glycine, and UV

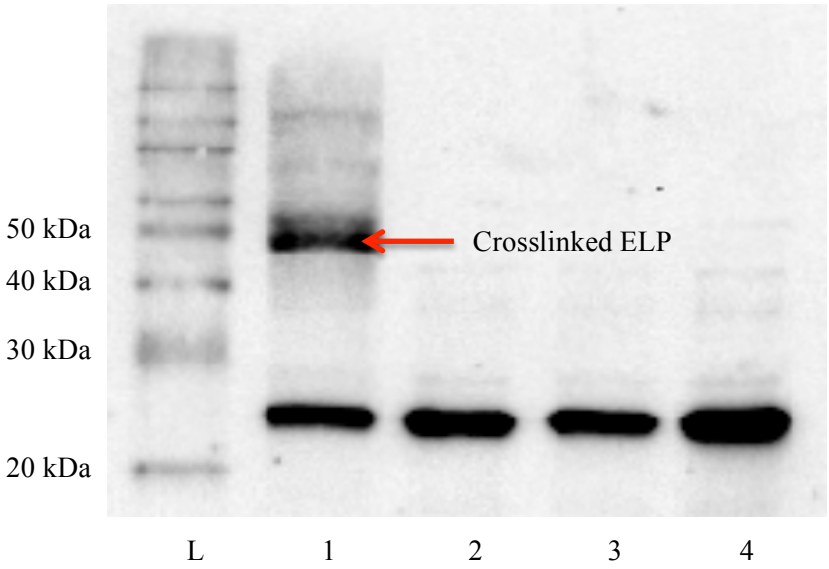

Figure 24 *In vivo* photocrosslinking of ELP. Leucine auxotrophic *E. coli* was cultured in M9 minimal media (All media contained valine, proline, and glycine) supplemented with photo-leucine or leucine. After exposure to UV light, western blot analysis was conducted using anti-FLAG to detect the presence of crosslinked ELP's.

3.4.3 Valine Induced ELP Expression

Table 5 Lane descriptions for Figure 25

Lane	Description
L	Biotin Ladder
1	1 mg Photoleucine
2	1 mg Leucine
3	No Amino Acids
4	1 mg Valine
5	1 mg Proline and Glycine

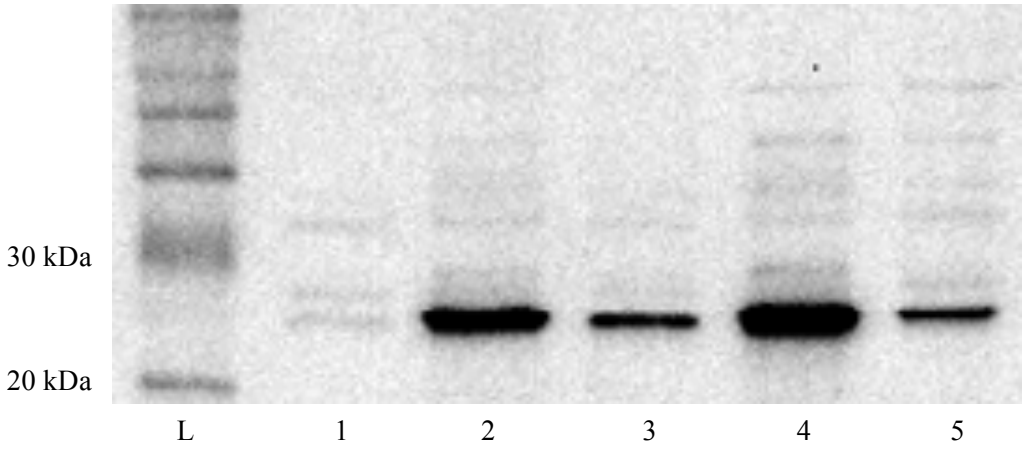

Figure 25 Increased ELP expression when growth media is supplemented with valine. M9 minimal media was supplemented with the described amino acids (Table 5) and inoculated for 24 hours for ELP expression.

To investigate the possibility that valine was enhancing ELP expression, a western blot was conducted on bacterial lysates from bacteria cultured in various expression medias for 6 hours. Figure 25 (above) shows the results of the western blot and Table 5 (above) defines the contents of the expression media used to culture bacteria. Bacteria cultured with leucine, valine, proline and glycine, and no additional amino acids expressed the ELP as evidenced by the protein band at 25 kDa; though, expression occured in different amounts. Bacteria cultured in the presence of proline and glycine, or no amino acids produced less ELP than those cultured in the

presence of leucine and valine. Futhermore, bacteria inoculated in the presence of valine had the highest amount of ELP expression, even more than bacteria cultured with leucine. The bacteria cultured with photoleucine produced the smallest quantity of ELP, just enough to register a signal.

3.4.4 Photoleucine Inhibits ELP Expression

Table 6 Lane descriptions for Figure 26

Lane	Description
L	Biotin Ladder
1	1 % glucose
2	0.5 mg Leucine
3	0.1 mg Photoleucine
4	0.5 mg Photoleucine
5	1 mg Photoleucine

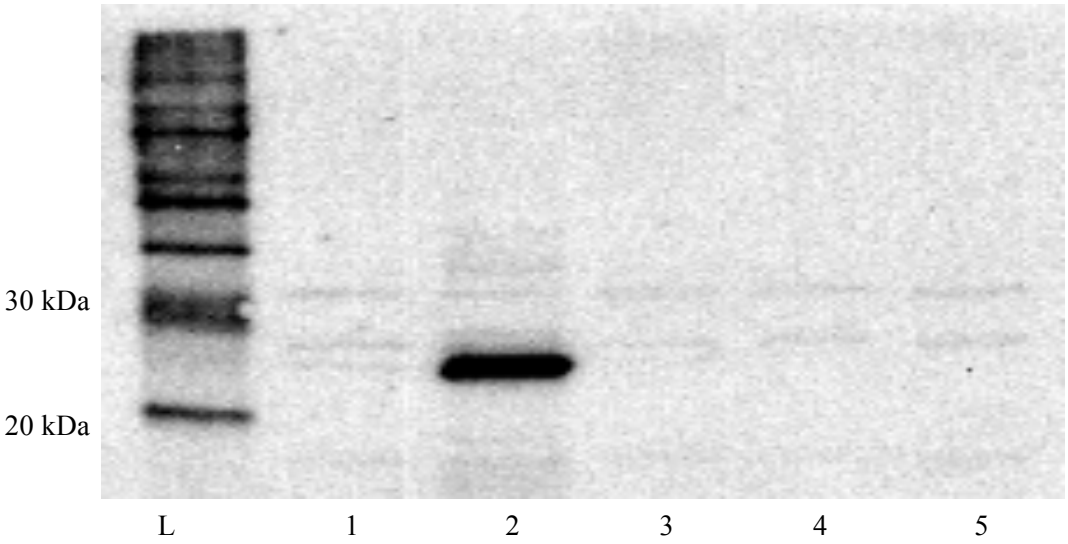

Figure 26 Addition of photoleucine to expression media reduces ELP expression. Leucine auxotrophic *E. coli* were cultured in M9 minimal media supplemented with the described amino acids (Table 6) for 24 hours.

To examine the effect of photoleucine on ELP expression, ELPs were expressed in M9 minimal media for 6 hours containing either leucine or various amounts of photoleucine. The

results of western blot analysis are presented in Figure 26 (previous page) and Table 6 (previous page) describes the expression media used to culture the bacteria that was used in each lane. Lane 1, containing the bacterial lysate from the overnight culture with 1% glucose, was used as a control to guarantee no ELP was being expressed while in TB media. As shown in the Figure 26, there was no ELP expression in the overnight starter culture. The only culture that appears to have expressed the ELP was the bacteria culture supplemented with leucine as indicated by the signal seen near 25 kDa, which is close to the approximate weight of the ELP monomers. When media containing 0.1 mg, 0.5 mg, and 1.0 mg of photoleucine was used for ELP expression, no ELP was expressed.

3.4.5 Optimization of the Leucine:Photoleucine Ratio in Expression Media

To determine the ratio of leucine:photoleucine that would be optimal for ELP expression, bacteria was cultured in M9 minimal media containing various ratios of leucine:photoleucine. ELP expression was induced for 6 hours. Results of the western blot analysis are exhibited in Figure 27 (next page), while the ratio of leucine:photoleucine used in expression media is described in Table 7 (next page). The overnight control bacteria cultured in 1% glucose did not produce any ELP, as expected. The bacteria cultured in media containing only photoleucine (Lane 2), did not express any ELP after inoculation; however, the remainder of the bacterial lysates did contain ELP. As demonstrated in Figure 25, the leucine:photoleucine ratios responsible for the highest amounts of ELP expression were the 1:30 ratio and 1:6 ratio. When ratios of 1:3 and 1:2 were used, ELP expression appears to have decreased slightly; though, it is not too significant. However, when a 1:1 ratio of leucine:photoleucine was used, there was a noticeable decrease in ELP expression when compared to other expression media that contained leucine and photoleucine.

Table 7 Leucine:photoleucine ratios for Figure 27

Lane	Description
L	Biotin Ladder
1	1 % glucose
2	0 mg Leucine
3	1:30 Ratio
4	1:6 Ratio
5	1:3 Ratio
6	1:2 Ratio
7	1:1 Ratio

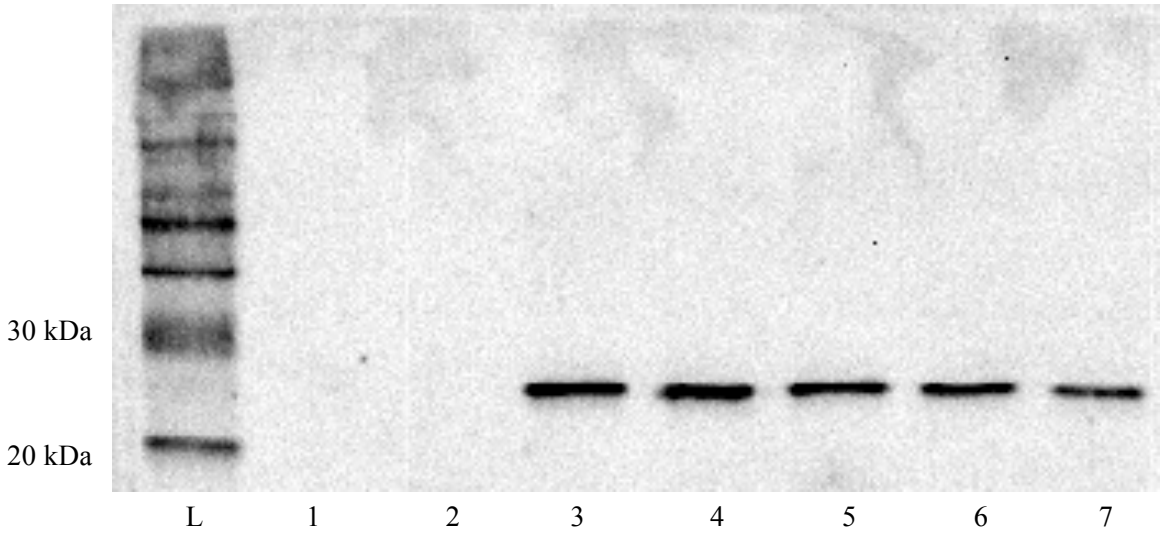

Figure 27 Increasing the leucine:photoleucine ratio decreases ELP expression. Leucine auxotrophic *E. coli* were cultured in M9 minimal media supplemented with the described amino acids (Table 7) for 24 hours.

3.5 Discussion

The original aim of this project was to create a photocrosslinkable ELP based hydrogel that could be synthesized in a single step (no need for conjugation, addition of crosslinking agents, or alteration of translational machinery) using photoreactive amino acid analogs. To start, we realized we needed to develop a protocol to culture leucine auxotrophic *E. coli* to levels

sufficient for ELP expression because standard M9 media containing supplemental amino acids was not conducive to bacteria growth. We achieved this using a combination of TB media, M9 media, and glucose. TB media was chosen for the starter culture because it provides a favorable environment for bacteria growth. Though, TB media contains high quantities of leucine, meaning bacteria should not express the ELP while in TB media since leucine will compete with photoleucine for incorporation into the ELP. To inhibit ELP expression, 1% glucose was added to the media because it has been shown the pET25b(+) expression system we used to express the ELP can be inhibited by the presence of 1% glucose [90]. Figure 21 demonstrates the addition of 1% glucose was able to inhibit ELP expression in TB media.

The TB media culture was then diluted in M9 media containing 1% glucose (1 : 20 dilution). The reason bacteria cultured in TB media was not centrifuged and immediately resuspended in the M9 expression media containing supplemental amino acids was we were aiming to reduce the possibility of leucine incorporation. Since TB media contains relatively large amounts of leucine, leucine may have been present in the cells directly following removal from TB media. Hence, dilution of the TB culture in M9 media containing 1% glucose for 24 hours allowed bacteria to use any excess leucine for the expression of other proteins while also supporting growth of bacteria to growth levels sufficient for ELP expression.

The bacteria present in the TB/M9 solution was then centrifuged, washed in PBS, centrifuged again, and resuspended in M9 expression media containing 0.2 % glycerol, supplemetal amino acids, and IPTG to induce ELP expression. This is the point at which photoleucine could be added to the expression media. Furthermore, valine, proline, and glycine were initially chosen as the constant supplemental amino acids because the ELP sequence contains large quantities of those three amino acids. It must be acknowledged the bacteria in the

expression media likely contained a small amount of excess leucine from the TB/M9 solution, but the amonut of leucine present was significantly reduced by the original dilution and resuspension in fresh M9 expression media.

Following induction with IPTG for 6 hours, bacteria was resuspended in PBS and exposed to UV light to promote photocrosslinking of ELP monomers. From Figure 24, it appears that photoactivation caused the formation of ELP dimers, showing the potentital for photocrosslinking ELP monomers and that the expression protocol devised allowed for the incorporation of photoleucine. However, there were two unanticipated finding. For one, the ELP was at a slightly higher molecular weight than anticipated; though, this could be attributed to aggregation of ELPs during SDS-PAGE analysis. Second, the western blot showed the largest quantity of ELP was produced when only valine, proline, and glycine were substituted into the expression media. This finding was unexpected because leucine auxotrophic *E. coli* were used as expression host. In theory, since the bacteria were not able to produce their own leucine, media not containing supplemental leucine should have had depressed levels of ELP expression since the ELP contains a relatively significant amount of leucine residues (40 leucine residues per ELP). However, it was found that bacteria cultured in media supplemented with valine, proline, glycine, and leucine produced a smaller quantity of ELP when compared to media not containing leucine. Even though it was not the original aim of the project, this phenomena was investigated further and it was hypothesized the addition of leucine to expression media may alter ELP expression; though, the mechanism by which this was happening was not understood.

To determine the effects of the supplemented amino acids on ELP expression, bacteria was cultured as discussed previously, but expression was carried out in media supplemented with either photoleucine, leucine, valine, or proline and glycine. Figure 25 demonstrates the

supplemented amino acids can cause ELP expression to vary. When ELP was expressed in media with proline and glycine or no amino acids, there was no significant difference in expression levels, suggesting the presence of proline and glycine does not alter ELP expression. Though, the presence of leucine or valine promotes ELP expression. Moreover, the data suggests the addition of valine to expression media enhances ELP expression when compared to leucine, supporting the data from Figure 24. Again, the reason for this is not understood because theoretically, leucine auxotrophic *E. coli* cultured in media without leucine should have minimal ELP expression levels due to the presence of leucine residues in the ELP sequence.

Also, the results from Figure 25 showed when photoleucine was the only amino acid added to expression media, ELP expression was reduced when compared to ELP expression in media containing supplemental amino acids or no additional amino acids. This was unexpected because, in theory, the bacteria being cultured in media without any supplemented amino acids should produce the smallest quantity of ELP relative to the expression media with supplemental amino acids. In addition, photoleucine had been reported to have no effects on protein expression and has been incorporated into eukaryotic proteins [85]. Hence, it was originally hypothesized the addition of photoleucine would produce the same expression levels as media supplemented with leucine and would be incorporated into ELPs. However, these results indicated photoleucine was reducing ELP expression.

To confirm whether or not photoleucine was impeding ELP expression, media containing various of amounts of photoleucine and a leucine control media were used for ELP expression. The results supported the claim that the presence of photoleucine was reducing ELP expression, regardless of the amount added to the media. Therefore, it was determined that in order for

photoreactive ELP expression to proceed, leucine or valine must be present in expression media alongside photoleucine.

It was decided leucine should be added with photoleucine even though this would theoretically increase competition for photoleucine incorporation, and ELP expression was higher in the presence of valine. The reason leucine was chosen over valine to be used in conjunction with photoleucine was we hypothesized valine might be incorporated preferentially over leucine due to the increased ELP expression seen in Figure 24 and Figure 25, even though the mechanism was not understood. If valine was incorporated preferentially over leucine, the use of valine with photoleucine may decrease the rate of photoleucine incorporation into the ELP. Hence, while leucine may decrease ELP expression in relation to valine, the rate of photoleucine incorporation may be increased. We intended to find a ratio of leucine:photoleucine that allowed for optimal ELP expression. The data in Figure 27 revealed if leucine and photoleucine are to be used as supplemental amino acids in the ELP expression media, ELP expression increases as the amount of leucine used is kept to a minimum. However, leucine is required for expression of the ELP.

When this investigation was started, it was hypothesized that by simply supplementing expression media with photoleucine and amino acids found in ELPs (valine, proline, and glycine), photoleucine would be incoporated into the ELP. While the *in vivo* crosslinking demonstrated it is possible, the same experiment caused us to question whether the expression protocol being used was efficient. As has been previously discussed, we found the addition of valine aids ELP expression in the leucine auxotrophic *E. coli* just as well, if not better, than leucine. We also noticed that ELP expression was significantly inhibited when photoleucine was

the sole supplemental amino acid. There are a number of explanations to explain these occurences.

Concerning ELP expression in the presence of photoleucine, even though photoleucine is not supposed to require the modification of translational machinery for incorporation due to the structural similarities to leucine, there may be a need to alter the leucine-tRNA synthetase (LeuRS) in the expression host. Tang and Tirrell demonstrated by replacing the threonine-252 residue in LeuRS with bulkier residues such as leucine, phenylalanine, or tyrosine, the proofreading capabilites of LeuRS were reduced, allowing for incorporation of noncanonical leucine analogs that could not be incorporated with unmodified LeuRS [88]. Another method could be to create a mutant LeuRS with an enlarged binding pocket. By enlarging the binding pocket of LeuRS, the specificity of LeuRS can be decreased; hence, increasing the incorporation of photoleucine. A similar strategy has been employed to incorporate phenylalanine analogs into recombinant proteins [20].

However, the specificity of the bacterial LeuRS may not be the reason for decreased ELP expression in the presence of photoleucine. From Figure 25, there was less ELP expressed in media containing photoleucine than in media containing no additional amino acids. This indicates not only is photoleucine not being incorporated into the ELP, but it is actually inhibiting ELP expression. Photoleucine could be having cytotoxic effects on the bacterial expression host, though this is unlikely as photoleucine has been shown to be noncytotoxic [85]. Another possible explanation for the apparent inhibition of ELP expression is photoleucine is being incorporated into proteins which are responsible for transcription of the ELP gene, and impairing their function. The finding that ELP expression occurs when even a minute amount of leucine is added to expression media with photoleucine hints this may be the problem as the

supplemental leucine could be incorporated into the necessary proteins, allowing them to function properly.

It was hypothesized leucine auxotrophic *E. coli* should not be able to produce ELP if only valine, proline, and glycine are added to expression media because of the lack of leucine. Our investigation reveals the addition of leucine to expression media does not enhance ELP expression, and may actually decrease ELP expression. The reasons for this are not quite clear. There is a possibility the bacterial LeuRS has undergone a mutation allowing valine to bypass the editing mechanisms of LeuRS. However, this would not explain the apparent increase in ELP expression when leucine is not added to the media. Another explanation is the possibility of errors being made while loading the SDS-PAGE gel. If a higher concentration of bacterial lysate was added for the bacteria cultured in leucine there may be a higher amount of ELP in the sample, causing an increase in signal strength.

Thus, we have created a photoreactive ELP that does not require the conjugation of functionalized moeities, addition of crosslinking agents, or manipulation of translational machinery to undergo photocrosslinking. While we were not able to synthesize a hydrogel, the potentital for hydrogel formation was demonstrated by the photocrosslinking of ELP monomers. Yet, we did find expression of the photoreactive ELP was not as straightforward as initially anticipated. Expression of the ELP and incorporation of photoleucine could not be conducted when photoleucine was the sole amino acid added to expression media. The mechanisms behind this are not completely understood; however, the specificity of the bacterial LeuRS could play a significant role. Additionally, we found ELP expression was able to take place at the same rate when valine or leucine was supplemented in expression media, possibly due to mutations in the LeuRS of the expression hosts. Understanding how the ELP expression protocol alters ELP

expression and photoleucine incorporation will be crucial to the future of this study as we aim to maximize the efficiency of photoreactive ELP production.

CHAPTER 4: THESIS CONCLUSION AND FUTURE WORK

In both studies, ELPs were used to create innovative drug delivery platforms to address various issues in regenerative medicine. In the first study, we produced an EGF-ELP fusion protein to aid in the delivery of exogenous EGF to chronic wounds. EGF is currently administered using simple bolus application techniques [32, 34]. These methods do not provide a means of protecting EGF from degradation in the chronic wound microenvironment or prevent diffusion of EGF away from the application site; hence, there is decreased bioavailability of EGF leading to insignificant improvements in tissue regeneration [32]. By fusing EGF with an ELP, we were able to combine the biological activity of EGF with the inverse phase transition abilities of ELPs. Since the fusion proteins aggregate at physiological temperatures, the EGF-ELP fusion protein can improve the bioavailability of EGF through the formation of localized drug depots at the application site. The EGF-ELP drug depots will not only increase the local concetration of EGF, but also minimize diffusion of EGF away from the injection site, thereby improving tissue regeneration. Future studies will need to be conducted in animal models to determine whether or not the EGF-ELP does improve chronic wound healing over free exogenouos EGF *in vivo*. Ultimately, we intend to conjugate the EGF-ELP to a hydrogel scaffold for drug delivery, allowing for the formation of an EGF concentration gradient to promote cell migration into the hydrogel.

The second portion of the thesis was meant to tackle many of the problems linked with hydrogel synthesis. As aforementioned, there have been a range of functionalized hydrogel platforms created that serve as drug carriers and structural scaffolds; though, many of these

platforms require the chemical conjugation of bioactive molecules and crosslinking domains to the hydrogel. This adds steps and time to hydrogel preparation, further complicating hydrogel production. Furthermore, many platforms cannot be injected and undergo gelation *in situ* because they utilize cytotoxic crosslinking reagents. We aimed to develop a photoreactive ELP based hydrogel platform that could deal with these issues. Photoresponsive ELPs were expressed using leucine auxotrophic *E. coli* that substitute photoleucine, a photoreactive leucine analog, for leucine throughout the ELP sequence. When exposed to UV light, photoleucine can covalently crosslink with nearby amino acid side chains and form a polymer network. The devised hydrogel platform allows for the synthesis of injectable hydrogels without the need for conjugation of crosslinking or bioactive moetieties.

In vivo crosslinking of photoreactive ELPs within the expression hosts showed the potential for the system. However, it was also found the addition of photoleucine alone to expression media inhibited ELP expression, and the addition of valine and leucine promoted ELP expression at the same rate. Hence, future studies will be needed to optimize expression media conditions for photoreactive ELP expression. Furthermore, there may be a need to modify the translational machinery of the leucine auxotrophic *E. coli*, in particular the LeuRS, if photoleucine cannot be incorporated into ELPs at a sufficient rate. Reducing the proofreading capability or increasing the size of the binding pocket of the LeuRS may lead to increased photoleucine incorporation [20, 88]. Also, the ELP will need to be purified, resuspended in aqueous solution, and photocrosslinked to confirm a hydrogel can be formed.

Once the photoreactive hydrogel has been fine-tuned for hydrogel formation, it could be used as a scaffold for the delivery of the EGF-ELP. Since the photoreactive ELP forms covalent crosslinks with any nearby amino acid side chain, the EGF-ELP can be immobilized to the

scaffold, potentially promoting cell migration into the scaffold and aiding in tissue regeneration. Investigations will need to be conducted to determine the biocompatibility of the hydrogel and the impact it has on the biological activity of the EGF-ELP. The combination of the EGF-ELP and photoreactive ELP hydrogel could prove to be a useful tool to aid in tissue regeneration.

REFERENCES

1. Keeley, F.W., C.M. Bellingham, and K.A. Woodhouse, *Elastin as a self-organizing biomaterial: use of recombinantly expressed human elastin polypeptides as a model for investigations of structure and self-assembly of elastin.* Philos Trans R Soc Lond B Biol Sci, 2002. **357**(1418): p. 185-9.
2. MacEwan, S.R. and A. Chilkoti, *Elastin-like polypeptides: biomedical applications of tunable biopolymers.* Biopolymers, 2010. **94**(1): p. 60-77.
3. Urry, D.W., *Free energy transduction in polypeptides and proteins based on inverse temperature transitions.* Prog Biophys Mol Biol, 1992. **57**(1): p. 23-57.
4. Urry, D.W., *Entropic elastic processes in protein mechanisms. II. Simple (passive) and coupled (active) development of elastic forces.* J Protein Chem, 1988. **7**(2): p. 81-114.
5. Urry, D.W., *Physical Chemistry of Biological Free Energy Transduction As Demonstrated by Elastic Protein-Based Polymers.* The Journal of Physical Chemistry B, 1997. **101**(51): p. 11007-11028.
6. Mi, L., *Molecular cloning of protein-based polymers.* Biomacromolecules, 2006. **7**(7): p. 2099-107.
7. Cappello, J., et al., *Genetic engineering of structural protein polymers.* Biotechnol Prog, 1990. **6**(3): p. 198-202.
8. McGrath, K.P., et al., *Genetically directed syntheses of new polymeric materials. Expression of artificial genes encoding proteins with repeating -(AlaGly)3ProGluGly- elements.* Journal of the American Chemical Society, 1992. **114**(2): p. 727-733.
9. McPherson, D.T., J. Xu, and D.W. Urry, *Product purification by reversible phase transition following Escherichia coli expression of genes encoding up to 251 repeats of the elastomeric pentapeptide GVGVP.* Protein Expr Purif, 1996. **7**(1): p. 51-7.
10. Meyer, D.E. and A. Chilkoti, *Purification of recombinant proteins by fusion with thermally-responsive polypeptides.* Nat Biotechnol, 1999. **17**(11): p. 1112-5.
11. Hage, D.S., *Affinity chromatography: a review of clinical applications.* Clin Chem, 1999. **45**(5): p. 593-615.
12. Urh, M., D. Simpson, and K. Zhao, *Chapter 26 Affinity Chromatography.* 2009. **463**: p. 417-438.
13. Matsumoto, R., et al., *Targeting of EGF-displayed protein nanoparticles with anticancer drugs.* J Biomed Mater Res B Appl Biomater, 2014. **102**(8): p. 1792-8.
14. Asai, D., et al., *Protein polymer hydrogels by in situ, rapid and reversible self-gelation.* Biomaterials, 2012. **33**(21): p. 5451-8.

15. Liu, W., et al., *Tumor accumulation, degradation and pharmacokinetics of elastin-like polypeptides in nude mice.* J Control Release, 2006. **116**(2): p. 170-8.

16. Betre, H., et al., *A thermally responsive biopolymer for intra-articular drug delivery.* J Control Release, 2006. **115**(2): p. 175-82.

17. Betre, H., et al., *Chondrocytic differentiation of human adipose-derived adult stem cells in elastin-like polypeptide.* Biomaterials, 2006. **27**(1): p. 91-9.

18. Koria, P., et al., *Self-assembling elastin-like peptides growth factor chimeric nanoparticles for the treatment of chronic wounds.* Proc Natl Acad Sci U S A, 2011. **108**(3): p. 1034-9.

19. McMillan, R.A. and V.P. Conticello, *Synthesis and Characterization of Elastin-Mimetic Protein Gels Derived from a Well-Defined Polypeptide Precursor.* Macromolecules, 2000. **33**(13): p. 4809-4821.

20. Carrico, I.S., et al., *Lithographic patterning of photoreactive cell-adhesive proteins.* J Am Chem Soc, 2007. **129**(16): p. 4874-5.

21. Cohen, S., *Isolation of a mouse submaxillary gland protein accelerating incisor eruption and eyelid opening in the new-born animal.* J Biol Chem, 1962. **237**: p. 1555-62.

22. Zeng, F. and R.C. Harris, *Epidermal growth factor, from gene organization to bedside.* Semin Cell Dev Biol, 2014. **28**: p. 2-11.

23. Tiaka, E.K., et al., *Epidermal growth factor in the treatment of diabetic foot ulcers: an update.* Perspect Vasc Surg Endovasc Ther, 2012. **24**(1): p. 37-44.

24. Savage, C.R., Jr. and S. Cohen, *Proliferation of corneal epithelium induced by epidermal growth factor.* Exp Eye Res, 1973. **15**(3): p. 361-6.

25. Franklin, J.D. and J.B. Lynch, *Effects of topical applications of epidermal growth factor on wound healing. Experimental study on rabbit ears.* Plast Reconstr Surg, 1979. **64**(6): p. 766-70.

26. Hori, K., et al., *Controlled-release of epidermal growth factor from cationized gelatin hydrogel enhances corneal epithelial wound healing.* J Control Release, 2007. **118**(2): p. 169-76.

27. Gonul, B., et al., *Effect of EGF on the corneal wound healing of alloxan diabetic mice.* Exp Eye Res, 1992. **54**(4): p. 519-24.

28. Kitazawa, T., et al., *The mechanism of accelerated corneal epithelial healing by human epidermal growth factor.* Invest Ophthalmol Vis Sci, 1990. **31**(9): p. 1773-8.

29. Brown, G.L., et al., *Enhancement of wound healing by topical treatment with epidermal growth factor.* N Engl J Med, 1989. **321**(2): p. 76-9.

30. Moseley, R., et al., *Extracellular matrix metabolites as potential biomarkers of disease activity in wound fluid: lessons learned from other inflammatory diseases?* Br J Dermatol, 2004. **150**(3): p. 401-13.

31. Harding, K.G., H.L. Morris, and G.K. Patel, *Science, medicine and the future: healing chronic wounds.* BMJ, 2002. **324**(7330): p. 160-3.

32. Falanga, V., et al., *Topical use of human recombinant epidermal growth factor (h-EGF) in venous ulcers.* J Dermatol Surg Oncol, 1992. **18**(7): p. 604-6.

33. Koria, P., *Delivery of growth factors for tissue regeneration and wound healing.* BioDrugs, 2012. **26**(3): p. 163-75.

34. Fernandez-Montequin, J.I., et al., *Intra-lesional injections of recombinant human epidermal growth factor promote granulation and healing in advanced diabetic foot ulcers: multicenter, randomised, placebo-controlled, double-blind study.* Int Wound J, 2009. **6**(6): p. 432-43.

35. Alemdaroglu, C., et al., *An investigation on burn wound healing in rats with chitosan gel formulation containing epidermal growth factor.* Burns, 2006. **32**(3): p. 319-27.

36. Shamji, M.F., et al., *Development and characterization of a fusion protein between thermally responsive elastin-like polypeptide and interleukin-1 receptor antagonist: sustained release of a local antiinflammatory therapeutic.* Arthritis Rheum, 2007. **56**(11): p. 3650-61.

37. Shamji, M.F., et al., *Synthesis and characterization of a thermally-responsive tumor necrosis factor antagonist.* J Control Release, 2008. **129**(3): p. 179-86.

38. MacEwan, S.R. and A. Chilkoti, *Applications of elastin-like polypeptides in drug delivery.* J Control Release, 2014. **190**: p. 314-30.

39. Bost, F., et al., *The JUN Kinase/Stress-activated Protein Kinase Pathway Is Required for Epidermal Growth Factor Stimulation of Growth of Human A549 Lung Carcinoma Cells.* Journal of Biological Chemistry, 1997. **272**(52): p. 33422-33429.

40. Gao, H., et al., *EGF enhances the migration of cancer cells by up-regulation of TRPM7.* Cell Calcium, 2011. **50**(6): p. 559-68.

41. Barnes, D.W., *Epidermal growth factor inhibits growth of A431 human epidermoid carcinoma in serum-free cell culture.* J Cell Biol, 1982. **93**(1): p. 1-4.

42. Schmidt, C.C., et al., *Effect of growth factors on the proliferation of fibroblasts from the medial collateral and anterior cruciate ligaments.* J Orthop Res, 1995. **13**(2): p. 184-90.

43. Carpenter, G. and S. Cohen, *Human epidermal growth factor and the proliferation of human fibroblasts.* J Cell Physiol, 1976. **88**(2): p. 227-37.

44. Chen, J.D., et al., *Epidermal growth factor (EGF) promotes human keratinocyte locomotion on collagen by increasing the alpha 2 integrin subunit.* Exp Cell Res, 1993. **209**(2): p. 216-23.

45. Bainbridge, P., *Wound healing and the role of fibroblasts.* J Wound Care, 2013. **22**(8): p. 407-8, 410-12.

46. Falanga, V., *Wound healing and its impairment in the diabetic foot.* Lancet, 2005. **366**(9498): p. 1736-43.

47. Yuan, Y. and P. Koria, *Proliferative activity of Elastin-like-Peptides Depends on Charge and Phase transition.* J Biomed Mater Res A, 2015.

48. Xu, X., et al., *Enhancing CNS repair in neurological disease: challenges arising from neurodegeneration and rewiring of the network.* CNS Drugs, 2011. **25**(7): p. 555-73.

49. Chen, F.M., M. Zhang, and Z.F. Wu, *Toward delivery of multiple growth factors in tissue engineering.* Biomaterials, 2010. **31**(24): p. 6279-308.

50. Margonar, R., et al., *Rehabilitation of atrophic maxilla using the combination of autogenous and allogeneic bone grafts followed by protocol-type prosthesis.* J Craniofac Surg, 2010. **21**(6): p. 1894-6.

51. Bukovcan, P. and J. Koller, *Treatment of partial-thickness scalds by skin xenografts--a retrospective study of 109 cases in a three-year period.* Acta Chir Plast, 2010. **52**(1): p. 7-12.

52. Fukumitsu, K., H. Yagi, and A. Soto-Gutierrez, *Bioengineering in organ transplantation: targeting the liver.* Transplant Proc, 2011. **43**(6): p. 2137-8.

53. Tompkins, R.G. and J.F. Burke, *Burn wound closure using permanent skin replacement materials.* World J Surg, 1992. **16**(1): p. 47-52.

54. Baiguera, S., B. D'Innocenzo, and P. Macchiarini, *Current status of regenerative replacement of the airway.* Expert Rev Respir Med, 2011. **5**(4): p. 487-94.

55. Wezel, F., J. Southgate, and D.F. Thomas, *Regenerative medicine in urology.* BJU Int, 2011. **108**(7): p. 1046-65.

56. Agrawal, V., et al., *Epimorphic regeneration approach to tissue replacement in adult mammals.* Proc Natl Acad Sci U S A, 2010. **107**(8): p. 3351-5.

57. Heddleston, J.M., et al., *Glioma stem cell maintenance: the role of the microenvironment.* Curr Pharm Des, 2011. **17**(23): p. 2386-401.

58. Davidson, J.M., *First-class delivery: getting growth factors to their destination.* J Invest Dermatol, 2008. **128**(6): p. 1360-2.

59. Patist, C.M., et al., *Freeze-dried poly(D,L-lactic acid) macroporous guidance scaffolds impregnated with brain-derived neurotrophic factor in the transected adult rat thoracic spinal cord.* Biomaterials, 2004. **25**(9): p. 1569-82.

60. Wikesjo, U.M., et al., *Periodontal repair in dogs: evaluation of a bioabsorbable space-providing macroporous membrane with recombinant human bone morphogenetic protein-2.* J Periodontol, 2003. **74**(5): p. 635-47.

61. Yang, F., et al., *The effect of incorporating RGD adhesive peptide in polyethylene glycol diacrylate hydrogel on osteogenesis of bone marrow stromal cells.* Biomaterials, 2005. **26**(30): p. 5991-8.

62. Nie, H., et al., *Three-dimensional fibrous PLGA/HAp composite scaffold for BMP-2 delivery.* Biotechnol Bioeng, 2008. **99**(1): p. 223-34.

63. Buxton, A.N., et al., *Design and characterization of poly(ethylene glycol) photopolymerizable semi-interpenetrating networks for chondrogenesis of human mesenchymal stem cells.* Tissue Eng, 2007. **13**(10): p. 2549-60.

64. Zhu, J. and R.E. Marchant, *Design properties of hydrogel tissue-engineering scaffolds.* Expert Rev Med Devices, 2011. **8**(5): p. 607-26.

65. Yoon, J.J., et al., *Heparin-immobilized biodegradable scaffolds for local and sustained release of angiogenic growth factor.* J Biomed Mater Res A, 2006. **79**(4): p. 934-42.

66. Jansen, R.G., et al., *FGF-2-loaded collagen scaffolds attract cells and blood vessels in rat oral mucosa.* J Oral Pathol Med, 2009. **38**(8): p. 630-8.

67. Ishimatsu, H., et al., *Formation of dentinal bridge on surface of regenerated dental pulp in dentin defects by controlled release of fibroblast growth factor-2 from gelatin hydrogels.* J Endod, 2009. **35**(6): p. 858-65.

68. Ishihara, M., et al., *Controlled releases of FGF-2 and paclitaxel from chitosan hydrogels and their subsequent effects on wound repair, angiogenesis, and tumor growth.* Curr Drug Deliv, 2006. **3**(4): p. 351-8.

69. Wu, J.C., et al., *Nerve repair using acidic fibroblast growth factor in human cervical spinal cord injury: a preliminary Phase I clinical study.* J Neurosurg Spine, 2008. **8**(3): p. 208-14.

70. Bessa, P.C., et al., *Thermoresponsive self-assembled elastin-based nanoparticles for delivery of BMPs.* J Control Release, 2010. **142**(3): p. 312-8.

71. Tang, D.W., et al., *Heparinized chitosan/poly(gamma-glutamic acid) nanoparticles for multi-functional delivery of fibroblast growth factor and heparin.* Biomaterials, 2010. **31**(35): p. 9320-32.

72. El-Sherbiny, I.M. and M.H. Yacoub, *Hydrogel scaffolds for tissue engineering: Progress and challenges.* Glob Cardiol Sci Pract, 2013. **2013**(3): p. 316-42.

73. Anal, A.K. and W.F. Stevens, *Chitosan-alginate multilayer beads for controlled release of ampicillin.* Int J Pharm, 2005. **290**(1-2): p. 45-54.

74. Kimura, T., et al., *Preparation of poly(vinyl alcohol)/DNA hydrogels via hydrogen bonds formed on ultra-high pressurization and controlled release of DNA from the hydrogels for gene delivery.* J Artif Organs, 2007. **10**(2): p. 104-8.

75. Wu, X., et al., *Alterations in physical cross-linking modulate mechanical properties of two-phase protein polymer networks.* Biomacromolecules, 2005. **6**(6): p. 3037-44.

76. Trabbic-Carlson, K., L.A. Setton, and A. Chilkoti, *Swelling and mechanical behaviors of chemically cross-linked hydrogels of elastin-like polypeptides.* Biomacromolecules, 2003. **4**(3): p. 572-80.

77. Sallach, R.E., et al., *Elastin-Mimetic Protein Polymers Capable of Physical and Chemical Crosslinking.* Biomaterials, 2009. **30**(3): p. 409-422.

78. Bozzini, S., et al., *Enzymatic cross-linking of human recombinant elastin (HELP) as biomimetic approach in vascular tissue engineering.* J Mater Sci Mater Med, 2011. **22**(12): p. 2641-50.

79. Ravi, S., et al., *Incorporation of fibronectin to enhance cytocompatibility in multilayer elastin-like protein scaffolds for tissue engineering.* Journal of biomedical materials research. Part A, 2013. **101**(7): p. 10.1002/jbm.a.34484.

80. Nettles, D.L., et al., *In situ crosslinking elastin-like polypeptide gels for application to articular cartilage repair in a goat osteochondral defect model.* Tissue Eng Part A, 2008. **14**(7): p. 1133-40.

81. Fan, Y., et al., *In situ forming hydrogels via catalyst-free and bioorthogonal "tetrazole-alkene" photo-click chemistry.* Biomacromolecules, 2013. **14**(8): p. 2814-21.

82. Raphel, J., A. Parisi-Amon, and S. Heilshorn, *Photoreactive elastin-like proteins for use as versatile bioactive materials and surface coatings.* J Mater Chem, 2012. **22**(37): p. 19429-19437.

83. Annabi, N., et al., *Engineered cell-laden human protein-based elastomer.* Biomaterials, 2013. **34**(22): p. 5496-505.

84. Ono, K., et al., *Experimental evaluation of photocrosslinkable chitosan as a biologic adhesive with surgical applications.* Surgery, 2001. **130**(5): p. 844-850.

85. Suchanek, M., A. Radzikowska, and C. Thiele, *Photo-leucine and photo-methionine allow identification of protein-protein interactions in living cells.* Nat Methods, 2005. **2**(4): p. 261-7.

86. Link, A.J., M.L. Mock, and D.A. Tirrell, *Non-canonical amino acids in protein engineering.* Curr Opin Biotechnol, 2003. **14**(6): p. 603-9.

87. Ibba, M., P. Kast, and H. Hennecke, *Substrate specificity is determined by amino acid binding pocket size in Escherichia coli phenylalanyl-tRNA synthetase.* Biochemistry, 1994. **33**(23): p. 7107-12.

88. Tang, Y. and D.A. Tirrell, *Attenuation of the editing activity of the Escherichia coli leucyl-tRNA synthetase allows incorporation of novel amino acids into proteins in vivo.* Biochemistry, 2002. **41**(34): p. 10635-45.

89. Baba, T., et al., *Construction of Escherichia coli K-12 in-frame, single-gene knockout mutants: the Keio collection.* Mol Syst Biol, 2006. **2**: p. 2006 0008.

90. Novy, R. and B. Morris, *Use of glucose to control basal expression in the pET System.* inNovations, 2001: p. 8-10.

APPENDIX A: AMINO ACID SEQUENCE FOR EGF AND ELP

Table A Sequence and molecular weight information for EGF and ELP

Protein	Sequence	Molecular Weight
EGF	*NSDSECPLSHDGYCLHDGVCMYIEALDKYAC NCVVGYIGERCQYRDLKWWELR*	6216 Da
ELP	$(VPGVG)_{40}[(VPGVG)_2(VPGCG)(VPGVG)_2]_2$	20496 Da
EGF-ELP	*NSDSECPLSHDGYCLHDGVCMYIEALDKYACNCVVGYIGERCQYRD LKWWELR* $(VPGVG)_{40}[(VPGVG)_2(VPGCG)(VPGVG)_2]_2$	26712 Da

APPENDIX B: FLAG-TAGGED EGF-ELP SIZE DATA

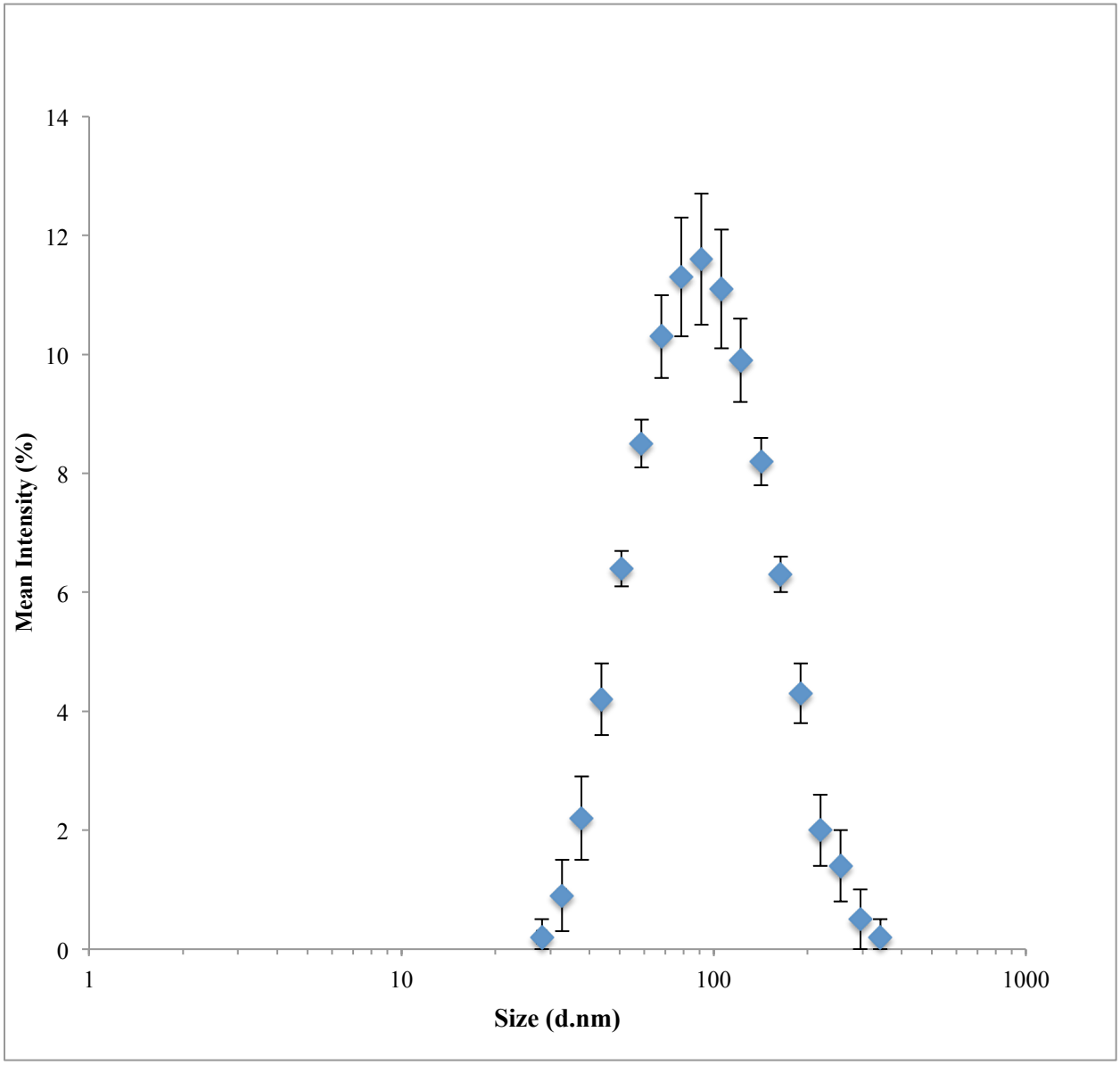

Figure A FLAG-tagged EGF-ELP particle size distribution at 4°C. The FLAG-tagged EGF-ELP was diluted in PBS to a concentration of 5 μM and analyzed at 4°C using DLS. Particle size distribution is represented as mean intensity (%). The Z-average was found to be 76.73 nm (data not shown).

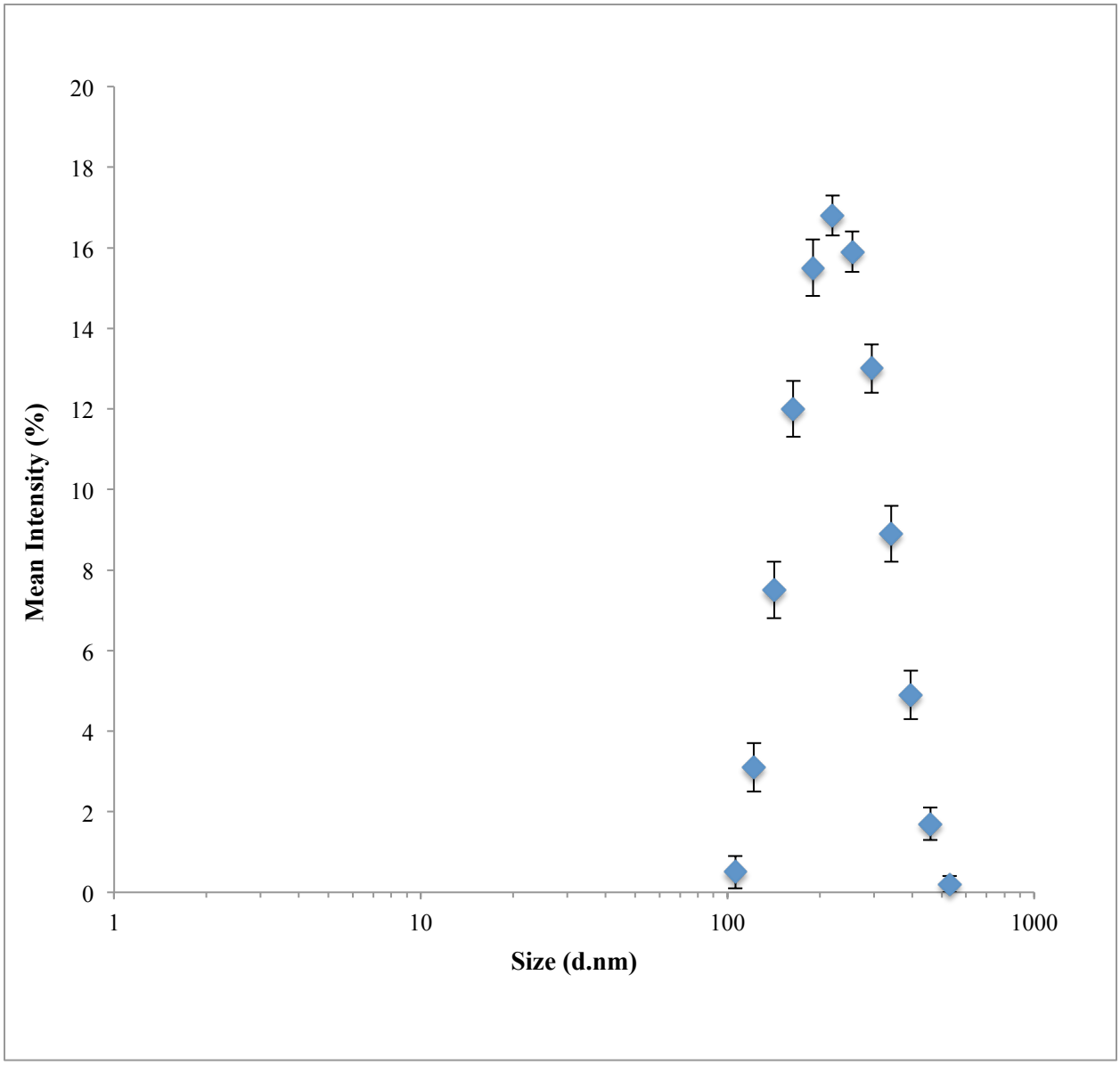

Figure B FLAG-tagged EGF-ELP particle size distribution at 37°C. The FLAG-tagged EGF-ELP was diluted in PBS to a concentration of 5 μM and analyzed at 37°C using DLS. Particle size distribution is represented as mean intensity (%). The Z-average of FLAG-tagged EGF-ELP aggregate was found to be 216.33 nm (data not shown).